[redacted]

[redacted]

NASA TECHNICAL MEMORANDUM

NASA TM X-3231

NASA TM X-3231

EFFECTS OF DIFFERENTIAL AND SYMMETRICAL AILERON DEFLECTION ON THE AERODYNAMIC CHARACTERISTICS OF AN NASA SUPERCRITICAL-WING RESEARCH AIRPLANE MODEL [redacted]

Dennis W. Bartlett

Langley Research Center
Hampton, Va. 23665

NATIONAL AERONAUTICS AND SPACE ADMINISTRATION • WASHINGTON, D. C. • OCTOBER 1975

[redacted]

[redacted]

1. Report No. NASA TM X-3231	2. Government Accession No.	3. Recipient's Catalog No.
4. Title and Subtitle EFFECTS OF DIFFERENTIAL AND SYMMETRICAL AILERON DEFLECTION ON THE AERODYNAMIC CHARACTERISTICS OF AN NASA SUPERCRITICAL-WING RESEARCH AIRPLANE MODEL (U)		5. Report Date October 1975 6. Performing Organization Code
7. Author(s) Dennis W. Bartlett		8. Performing Organization Report No. L-10220 10. Work Unit No. 505-11-11-04
9. Performing Organization Name and Address NASA Langley Research Center Hampton, Va. 23665		11. Contract or Grant No. 13. Type of Report and Period Covered Technical Memorandum
12. Sponsoring Agency Name and Address National Aeronautics and Space Administration Washington, D.C. 20546		14. Sponsoring Agency Code

15. Supplementary Notes

16. Abstract

An investigation has been conducted in the Langley 8-foot transonic pressure tunnel to determine the effects of differential and symmetrical aileron deflection on the longitudinal and lateral-directional aerodynamic characteristics of an 0.087-scale model of an NASA supercritical-wing research airplane (TF-8A). Tests were conducted at Mach numbers from 0.25 to 0.99 in order to determine the effects of differential aileron deflection and at Mach numbers of 0.25 and 0.50 to determine the effects of symmetrical aileron (flap) deflection. The angle-of-attack range for all tests varied from approximately -12° to 20°.

17. Key Words (Suggested by Author(s))
TF-8A supercritical wing research airplan
Lateral controls on supercritical wing

19. Security Classif. (of this report)	20. Security C
[redacted]	Uncla

EFFECTS OF DIFFERENTIAL AND SYMMETRICAL AILERON DEFLECTION ON THE AERODYNAMIC CHARACTERISTICS OF AN NASA SUPERCRITICAL-WING RESEARCH AIRPLANE MODEL (U)

Dennis W. Bartlett
Langley Research Center

SUMMARY

An investigation has been conducted in the Langley 8-foot transonic pressure tunnel to determine the effects of differential and symmetrical aileron deflection on the longitudinal and lateral-directional aerodynamic characteristics of an 0.087-scale model of an NASA supercritical-wing research airplane (TF-8A). Tests were conducted at Mach numbers from 0.25 to 0.99 in order to determine the effects of differential aileron deflection and at Mach numbers of 0.25 and 0.50 to determine the effects of a symmetrical aileron (flap) deflection. The angle-of-attack range for all tests varied from approximately -12° to 20°.

For a differential aileron deflection to 30°, positive roll-control effectiveness is indicated throughout the angle-of-attack and Mach number ranges. When symmetrically deflected, the ailerons provide positive flap effectiveness values of about 0.011 per degree at an angle of attack of 0° and about 0.007 per degree at an angle of attack of 8.5° (the limiting angle for take-off and landing) at Mach numbers of 0.25 and 0.50.

Flap effectiveness values for the 20° effective flap deflection in combination with 10° of differential aileron ($\delta'_{a,L} = 15°$, $\delta'_{a,R} = 25°$) are slightly lower than for the basic 20° symmetrically deflected case. In addition, the roll-control effectiveness for this configuration ($\delta'_{a,L} = 15°$, $\delta'_{a,R} = 25°$) is slightly lower than that for the 10° differential aileron deflection alone.

INTRODUCTION

An early flight demonstration of the NASA supercritical airfoil concept involved the testing of an advanced transport-configured wing on a U.S. Navy fighter aircraft (TF-8A) employed as a test bed. (See refs. 1 to 8.) Since verification of wind-tunnel performance results was of primary interest in the flight-test program, the lateral controls were designed to be relatively simple to construct and operate but yet provide sufficient flight safety to allow for the exploration of both the buffet boundary and the simulated upset,

overspeed case. In addition, the lateral controls (ailerons) were configured for a symmetrical deflection capability to permit their use as flaps for take-off and landing, and thereby reduce take-off and landing speeds. Although the lateral-control system is not typical of that used on current transport-type aircraft, these results represent some of the first available with respect to the application of lateral controls to a supercritical wing.

Early wind-tunnel tests to determine roll-control effectiveness and aileron hinge moments (ref. 8) were conducted by moving the aileron on one side only in order that separate effects of the up-moving and down-moving aileron could be obtained. The present paper presents results of a subsequent investigation for a near-final version of the research airplane in which the roll-control effectiveness for differential aileron deflection was obtained, and at the lower Mach numbers of these tests, limited effects of symmetrical aileron deflection were obtained to determine their effectiveness as flaps. The investigation was conducted in the Langley 8-foot transonic pressure tunnel at Mach numbers from 0.25 to 0.99 and over an angle-of-attack range that extended from about -12° to 20°. Test Reynolds numbers varied from approximately 14×10^6 per meter at 0.50 Mach number to 10×10^6 per meter at a Mach number of 0.99.

SYMBOLS

Results presented herein are referred to the body-axis system for the lateral and directional aerodynamic characteristics and to the stability-axis system for the longitudinal aerodynamic characteristics. Force and moment data have been reduced to conventional coefficient form based on the geometry of the reference wing planform; that is, the planform produced by extending the straight leading and trailing edges of the outboard sections of the wing to the fuselage center line. (See fig. 1.) Moments are referenced to the quarter-chord point (fuselage station 99.45 cm (39.155 in.)) of the mean geometric chord of the reference wing panel. All dimensional values are given in both SI and U.S. Customary Units; however, measurements and calculations were made in U.S. Customary Units.

Coefficients and symbols used herein are defined as follows:

b wing span, 114.30 cm (45.000 in.)

C_D drag coefficient, $\frac{\text{Drag}}{qS}$

C_L lift coefficient, $\frac{\text{Lift}}{qS}$

$C_{L,o}$ lift coefficient at zero angle of attack

C_l rolling-moment coefficient, $\frac{\text{Rolling moment}}{qSb}$

C_m pitching-moment coefficient, $\frac{\text{Pitching moment}}{qS\bar{c}}$

$C_{m,o}$ pitching-moment coefficient at zero lift coefficient

C_n yawing-moment coefficient, $\frac{\text{Yawing moment}}{qSb}$

C_Y side-force coefficient, $\frac{\text{Side force}}{qS}$

c local streamwise chord of wing

$\bar{c}$ mean geometric chord of reference wing panel, 18.087 cm (7.121 in.), defined as $\frac{b}{S}\int_0^1 c^2 d\left(\frac{y}{b/2}\right)$

M free-stream Mach number

q free-stream dynamic pressure, N/m^2 (lb/ft^2)

S area of reference wing planform including fuselage intercept, 0.193 m^2 (2.075 ft^2)

y spanwise distance measured normal to model plane of symmetry

α angle of attack referred to a model water line, deg

Δ incremented value from zero control deflection

$\frac{\Delta C_D}{\Delta \delta_f}$ effect of flap (symmetrical aileron) deflection on drag coefficient per deg

$\frac{\Delta C_L}{\Delta \delta_f}$ effect of flap (symmetrical aileron deflection) on lift coefficient (flap effectiveness parameter) per deg

$\frac{\Delta C_l}{\Delta \delta_a}$ effect of differential aileron deflection on rolling-moment coefficient (aileron or roll-control effectiveness parameter) per deg

$\frac{\Delta C_m}{\Delta \delta_f}$ effect of flap (symmetrical aileron) deflection on pitching-moment coefficient per deg

$\frac{\Delta C_n}{\Delta \delta_a}$ effect of differential aileron deflection on yawing-moment coefficient per deg

$\frac{\Delta C_Y}{\Delta \delta_a}$ effect of differential aileron deflection on side-force coefficient per deg

δ_a differential aileron deflection, $\delta'_{a,R} - \delta'_{a,L}$, deg

δ'_a deflection of either aileron, positive for trailing edge down, deg

δ_f flap (symmetrical aileron) deflection, $\delta'_{a,L} = \delta'_{a,R}$, deg

δ_h horizontal tail deflection angle (positive when trailing edge is down), deg

Subscripts:

L left control

R right control

APPARATUS AND PROCEDURES

Model Description

Geometric characteristics of the 0.087-scale research airplane model are presented in figure 1 and photographs of the model are presented in figure 2. The basic fuselage and tail surfaces are scaled versions of those of the test-bed aircraft (TF-8A). The model fuselage was equipped with flow-through ducts which discharge at the base of

the model on either side of a flat-sided model support sting. The aft section of the flow-through ducts used in the present investigation had smaller exit areas than ducts used in most of the previous wind-tunnel investigations (refs. 2 to 6); however, they do correspond to those used in references 7 and 8. The smaller duct exits provided increased clearance between the sides of the ducts and sting for lateral-directional stability tests.

The wing, which was constructed of aluminum, was mounted with a root incidence angle of 1.5° and had approximately 5.5° of twist (washout) in the unloaded condition. The reference wing panel (fig. 1(a)) has an aspect ratio of 6.78, a taper ratio of 0.364, and the quarter-chord line swept back 42.24°. The area of the reference wing planform including the fuselage intercept is 0.193 m^2 (2.075 ft^2), and the mean geometric chord of the reference wing panel is 18.087 cm (7.121 in.). The wing section coordinates are identical to those presented in reference 2.

An underwing, leading-edge vortex generator (discussed in refs. 4 and 7 and shown in fig. 1(c)) was included on each wing panel at the 60-percent semispan station. It should be noted that the vortex generators were not used on the wing for the lateral-control tests reported in reference 8.

The ailerons extended from the 40- to 80-percent semispan stations and had chord lengths equal to 25 percent of the local streamwise chords. The ailerons were hinged about the 75-percent chord line, and each had an area of 87.80 cm^2 (13.61 in^2) and a span of 22.86 cm (9.00 in.). (See fig. 1(b).) Each aileron deflection angle was set with an angle bracket and care was taken to seal the gap between the aileron and wing along the hinge line with silicone rubber. The ailerons on the full-scale airplane were also sealed along the hinge line to prevent air leaking from the wing lower surface to the upper surface which could cause the flow to separate over the aileron.

Test Facility

The Langley 8-foot transonic pressure tunnel (ref. 9) is a single-return, continuous-flow, rectangular, slotted-throat wind tunnel with controls that allow for the independent variation of Mach number, stagnation pressure, temperature, and dewpoint. The stagnation temperature of the tunnel air was automatically maintained at approximately 322 K (120° F), and the air was dried sufficiently to preclude significant condensation effects. (See ref. 10.) The upper and lower walls of the test section are axially slotted to permit testing through the transonic speed range. The regular tunnel slots, which produce an average open ratio per slotted wall of 0.06, were replaced for the present investigation by slots which increased the open ratio to 0.22. These latter slots, designed on the basis of reference 11, were used to minimize the blockage effects caused by the relatively large model.

Measurements and Test Conditions

Measurements of overall forces and moments on the model were obtained by using a six-component, electrical strain-gage balance housed within the fuselage cavity. Differential-pressure transducers referenced to free-stream static pressure were used to measure the pressure in the fuselage balance chamber and at the model base.

Boundary-layer-trip arrangements for the wing are shown in figure 3. Transition strips were also applied to the horizontal and vertical tails at 5 percent of the local streamwise chord by using 0.127-cm-wide (0.05-in.) strips of No. 120 carborundum grit set in a plastic adhesive. Similar strips were located 2.54 cm (1.0 in.) rearward of the model nose and inlet lip, and an additional strip was placed on the inner surface of the inlet 1.27 cm (0.5 in.) rearward of the inlet lip.

Results presented herein were obtained by using two support arrangements downstream of the model sting. In addition to the normal straight-sting arrangement, it was necessary to use an offset coupling (fig. 1(d)) to obtain the higher angle-of-attack results. The coupling offset the model sting vertically below the normal model support and allowed for angles of attack to approximately 24° with the 9° angle-of-attack adapter installed.

Tests were conducted at Mach numbers from 0.25 to 0.99 in order to determine the effects of differential aileron deflection and at Mach numbers of 0.25 and 0.50 to determine the effects of symmetrical aileron (flap) deflection. All tests were conducted for a sideslip angle of 0° and with the horizontal tail deflected -2.5° (leading edge down). Specific tunnel conditions for the present investigation are presented in the following table:

Mach number	Temperature		Reynolds number for –			
			Straight sting		Offset sting	
	K	°F	Per meter	Per foot	Per meter	Per foot
0.99	322	120	10.5×10^6	3.2×10^6	---------	--------
.95	322	120	10.8	3.3	8.6×10^6	2.7×10^6
.90	322	120	11.8	3.6	9.2	2.8
.80	322	120	12.8	3.9	9.8	3.0
.50	322	120	14.4	4.4	14.4	4.4
.25	322	120	9.8	3.0	9.8	3.0

Corrections

Drag coefficients contained herein have been adjusted to a condition corresponding to free-stream static pressure acting in the balance chamber and at the model base (excluding the duct exit areas). No adjustments have been made for the internal duct drag; however, internal drag coefficients and mass-flow ratios are contained in reference 8.

Corrections have been made to the measured angles of attack to account for deflection of the model balance and sting support system under aerodynamic load, for tunnel airflow angularity, and for the first-order boundary-induced lift-interference effects as calculated from the theory of reference 12. This last correction amounts to a reduction in the measured angle of attack by 0.24 multiplied by the normal-force coefficient.

PRESENTATION OF RESULTS

The results obtained by using the offset-coupling-sting arrangement (fig. 1(d)) are indicated by crossed symbols in the figures, and some differences due to the interference pressure field of the offset coupling may be noted over the angle-of-attack range where the data from the two sting arrangements overlap. Also note (see table in section "Measurements and Test Conditions") that the offset-coupling data were obtained at slightly lower Reynolds numbers at all Mach numbers except 0.25 and 0.50.

The following is a list of figures presenting results of this investigation. Note that in the summary figures, data obtained with the offset-coupling-sting arrangement were used at angles of attack above 12°.

DISCUSSION OF RESULTS

Aerodynamic Characteristics With Differential Aileron Deflection

Longitudinal aerodynamics.- The effect of differential-aileron deflection on the longitudinal aerodynamic coefficients is presented in figure 4. (Note that these data are plotted with sliding scales.) Except for the lowest Mach numbers tested (0.25 and 0.50), there is an increasingly negative $C_{L,o}$ shift and a correspondingly positive $C_{m,o}$ shift with increasing differential aileron deflection. These effects apply to all conditions except $\delta'_{a,L} = 15^o$, $\delta'_{a,R} = 25^o$ which is an effective flap deflection of 20^o with 10^o of differential aileron deflection. These effects on the longitudinal aerodynamic characteristics due to differential aileron deflection are a result of the "up-moving" aileron being roughly twice as effective in decreasing lift as the "down-moving" aileron is in generating lift. This statement is based on the results of reference 8 in which the independent effects of the "up-moving" and "down-moving" aileron are documented.

Although pitch-up is indicated at all Mach numbers of figure 4, the model is stable up to lift coefficients of more than twice that required for cruise ($C_L \approx 0.40$); in addition, neither the point at which pitch-up occurs nor the severity of pitch-up is appreciably affected by differential aileron deflections to 30^o. (See fig. 4.)

As would be expected, there is an increase in the minimum drag with increasing differential aileron deflection at all the Mach numbers for which data are presented in figure 4. Care should be exercised in any comparison of the drag results contained herein with other drag results obtained with this model since two sizes of exit ducts were utilized for the various investigations as pointed out in the section entitled "Model Description."

Lateral-directional aerodynamics.- The effect of differential aileron deflection on the lateral-directional aerodynamic coefficients is presented in figure 5, and the lateral-directional aileron-control parameters are presented in figures 6 and 7 as a function of angle of attack and Mach number, respectively. The offsets in C_l, C_n, and C_Y for $\delta_a = 0$ in figure 5 are due to model asymmetry.

Positive roll-control effectiveness $\left(\text{negative } \frac{\Delta C_l}{\Delta \delta_a} \text{ values}\right)$ is indicated throughout the angle-of-attack and Mach number ranges of the investigation whereas only small changes in directional stability due to differential-aileron deflection are noted. The apparent aileron reversal at a Mach number of 0.25 near an angle of attack of 18° (fig. 6(a)) is probably a result of asymmetric wing stall associated with model assymmetry and should not be considered as actual aileron reversal. Note that the basic configuration with no aileron deflection also exhibits relatively large positive rolling moments near an angle of attack of 18° (fig. 5(a)). It should also be pointed out that the maximum angle of attack for take-off and landing is limited to 8.5° for this configuration because of ground-clearance considerations.

Roll-control effectiveness is essentially constant with increasing differential aileron deflection (δ_a = 10° to 30°) except for the condition with 10° of differential aileron in combination with 20° effective flap deflection $\left(\delta'_{a,L} = 15°, \quad \delta'_{a,R} = 25°\right)$ which produces less positive roll-control effectiveness than for the basic 10° of differential aileron deflection alone $\left(\delta'_{a,L} = -5°, \quad \delta'_{a,R} = 5°\right)$. This is a probable result of increased separation associated with the "down-moving" aileron.

In general, the roll-control effectiveness $\left(\frac{\Delta C_l}{\Delta \delta_a}\right)$ is maximum between angles of attack of 0° and 4° and decreases with changes in angle of attack in either the positive or negative direction (fig. 6), and for a constant angle of attack, roll-control effectiveness is relatively constant with Mach number (fig. 7).

The rather sharp variations in rolling moment noted in the results of figure 5 are primarily associated with asymmetric wing stall and occur near the angles of attack at which pitch-up is also indicated. In addition, the relatively large positive pressure field from the offset coupling in conjunction with the separated flow conditions at high angles of attack are probably responsible for the differences in the overlapping data from the straight- and offset-coupling-sting arrangements.

Longitudinal Aerodynamic Characteristics

With Symmetrical Aileron Deflection

The effects of symmetrical aileron (flap) deflection on the longitudinal characteristics are presented in figure 8 and summarized in figure 9 for Mach numbers of 0.25 and 0.50. Also shown are the effects of ±5° aileron deflection (10° differential) in combination with 20° effective flap deflection $\left(\delta'_{a,L} = 15°, \quad \delta'_{a,R} = 25°\right)$.

The flap effectiveness $\frac{\Delta C_L}{\Delta \delta_f}$ is seen to remain fairly constant for Mach numbers between 0.25 and 0.50 for a given angle of attack (fig. 9), but decreases with an increase

in angle of attack from a value of about 0.011 per degree at $\alpha = 0^o$ to about 0.007 at $\alpha = 8.5^o$, the limiting angle for take-off and landing for this configuration. Flap effectiveness for 20° flap deflection is slightly higher than for the 15° deflected case throughout the angle-of-attack range at both 0.25 and 0.50 Mach numbers; however, flap effectiveness for the 20° effective-flap condition $(\delta'_{a,L} = 15^o, \ \delta'_{a,R} = 25^o)$ is not as large as for either the 15° or 20° symmetrically deflected conditions. (See fig. 9.) This loss in effectiveness, as mentioned earlier, is probably a result of the "up-moving" aileron being more effective than the "down-moving" aileron.

As would be expected, flap deflections to 20° are accompanied by significant drag increases (34 percent) at lift coefficients near $C_L = 0$. At lift coefficients near those for take-off and landing $(C_L \approx 0.8)$, little or no drag increase due to flap deflection is apparent (fig. 8); however, the present data are for untrimmed conditions $(\delta_h = -2.5^o)$. The results of reference 13 (obtained with the same model) indicate that the negative pitching moments associated with the 20° flap deflection (fig. 8) can be trimmed for take-off and landing conditions by using a horizontal-tail angle of approximately -10° and a center of gravity located at the 25-percent point of the mean geometric chord. In addition, a comparison of the present data (fig. 8(a)) with those of figure 4(a) in reference 13 shows an increase in drag coefficient of about 0.0130 as a result of trimming the 20° flap configuration near a lift coefficient of 0.8.

SUMMARY OF RESULTS

The present wind-tunnel investigation of differential and symmetrical aileron deflection for an NASA supercritical-wing research airplane (TF-8A) has shown the following results:

1. For differential-aileron deflection to 30°, positive roll-control effectiveness is indicated throughout the angle-of-attack and Mach number ranges of the investigation.

2. When symmetrically deflected, the ailerons provide positive flap effectiveness values of about 0.011 per degree at an angle of attack of 0° and about 0.007 per degree at an angle of attack of 8.5° (take-off and landing angle) at both Mach numbers of 0.25 and 0.50.

3. Flap effectiveness values for the 20° effective flap deflection in combination with 10° of differential aileron deflection $(\delta'_{a,L} = 15^o, \ \delta'_{a,R} = 25^o)$ are slightly lower than for the 20° symmetrically deflected condition. In addition, the roll-control effectiveness for

this configuration $\left(\delta'_{a,L} = 15^{o}, \quad \delta'_{a,R} = 25^{o}\right)$ is slightly lower than for 10^{o} of differential aileron deflection alone.

Langley Research Center
National Aeronautics and Space Administration
Hampton, Va. 23665
August 28, 1975

REFERENCES

1. Supercritical Wing Technology – A Progress Report on Flight Evaluations. NASA SP-301, 1972.

2. Bartlett, Dennis W.; and Re, Richard J.: Wind-Tunnel Investigation of Basic Aerodynamic Characteristics of a Supercritical-Wing Research Airplane Configuration. NASA TM X-2470, 1972.

3. Harris, Charles D.: Wind-Tunnel Measurements of Aerodynamic Load Distribution on an NASA Supercritical-Wing Research Airplane Configuration. NASA TM X-2469, 1972.

4. Harris, Charles D.; and Bartlett, Dennis W.: Wind-Tunnel Investigation of Effects of Underwing Leading-Edge Vortex Generators on a Supercritical-Wing Research Airplane Configuration. NASA TM X-2471, 1972.

5. Bartlett, Dennis W.; and Harris, Charles D.: Aerodynamic Characteristics of an NASA Supercritical-Wing Research Airplane Model With and Without Fuselage Area-Rule Addition at Mach 0.25 to 1.00. NASA TM X-2633, 1972.

6. Harris, Charles D.; and Bartlett, Dennis W.: Tabulated Pressure Measurements on an NASA Supercritical-Wing Research Airplane Model With and Without Fuselage Area-Rule Additions at Mach 0.25 to 1.00. NASA TM X-2634, 1972.

7. Bartlett, Dennis W.; Harris, Charles D.; and Kelly, Thomas C.: Wind-Tunnel Development of Underwing Leading-Edge Vortex Generators on an NASA Supercritical-Wing Research Airplane Configuration. NASA TM X-2808, 1973.

8. Re, Richard J.: Stability and Control Characteristics, Including Aileron Hinge Moments, of a Model of a Supercritical-Wing Research Airplane. NASA TM X-2929, 1974.

9. Schaefer, William T., Jr.: Characteristics of Major Active Wind Tunnels at the Langley Research Center. NASA TM X-1130, 1965.

10. Jordan, Frank L., Jr.: Investigation at Near-Sonic Speed of Some Effects of Humidity on the Longitudinal Aerodynamic Characteristics of an NASA Supercritical-Wing Research Airplane Model. NASA TM X-2618, 1972.

11. Davis, Don D., Jr.; and Moore, Dewey: Analytical Study of Blockage- and Lift-Interference Corrections for Slotted Tunnels Obtained by the Substitution of an Equivalent Homogeneous Boundary for the Discrete Slots. NACA RM L53E07b, 1953.

12. Wright, Ray H.; and Barger, Raymond L.: Wind-Tunnel Lift Interference on Swept-back Wings in Rectangular Test Sections With Slotted Top and Bottom Walls. NASA TR R-241, 1966.

13. Bartlett, Dennis W.; and Sangiorgio, Giuliana: Effects of Landing Gear, Speed Brake and Protuberances on the Longitudinal Aerodynamic Characteristics of an NASA Supercritical-Wing Research Airplane Model. NASA TM X-72684, 1975.

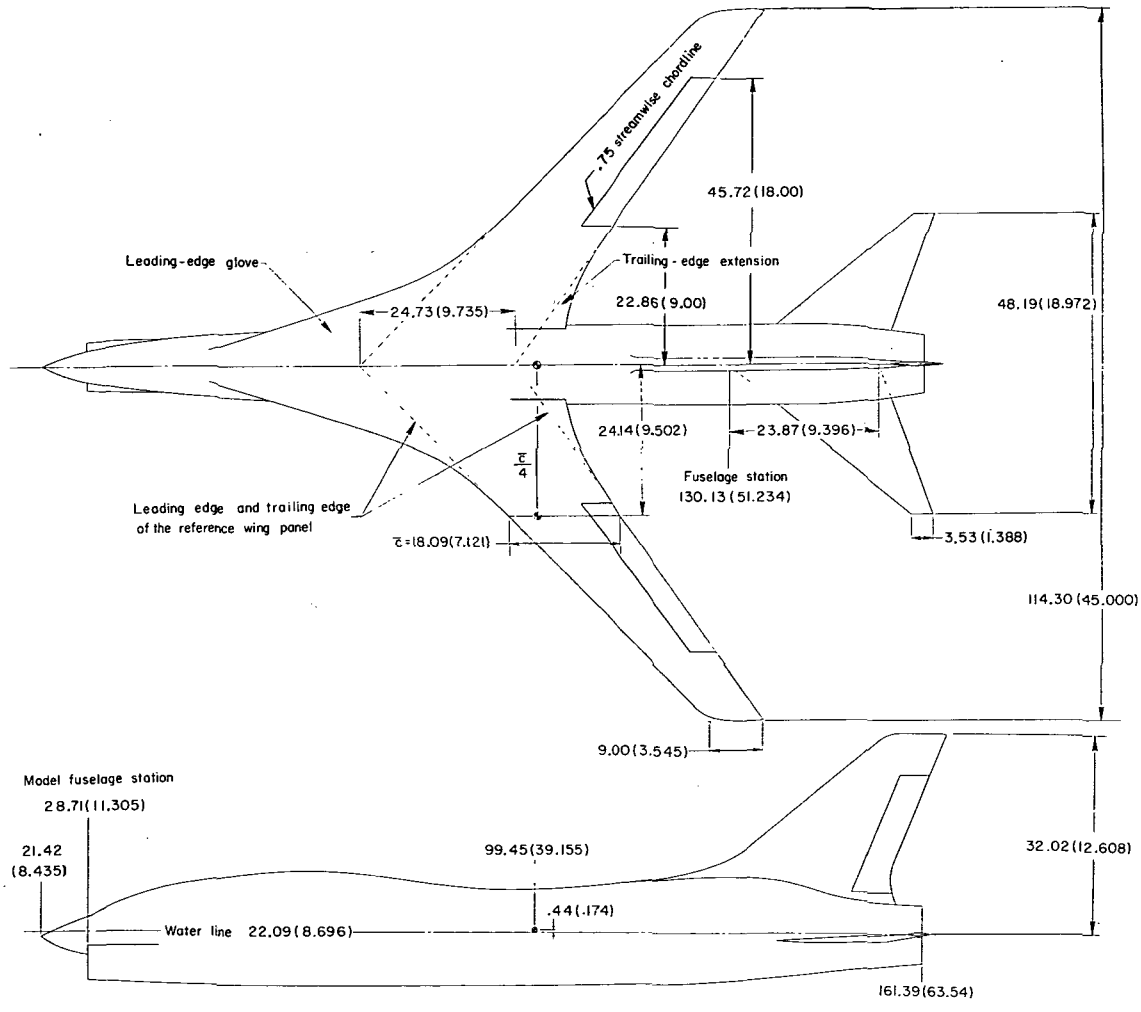

(a) General arrangement of the 0.087-scale model.

Figure 1.- Model details. Dimensions are in centimeters (inches).

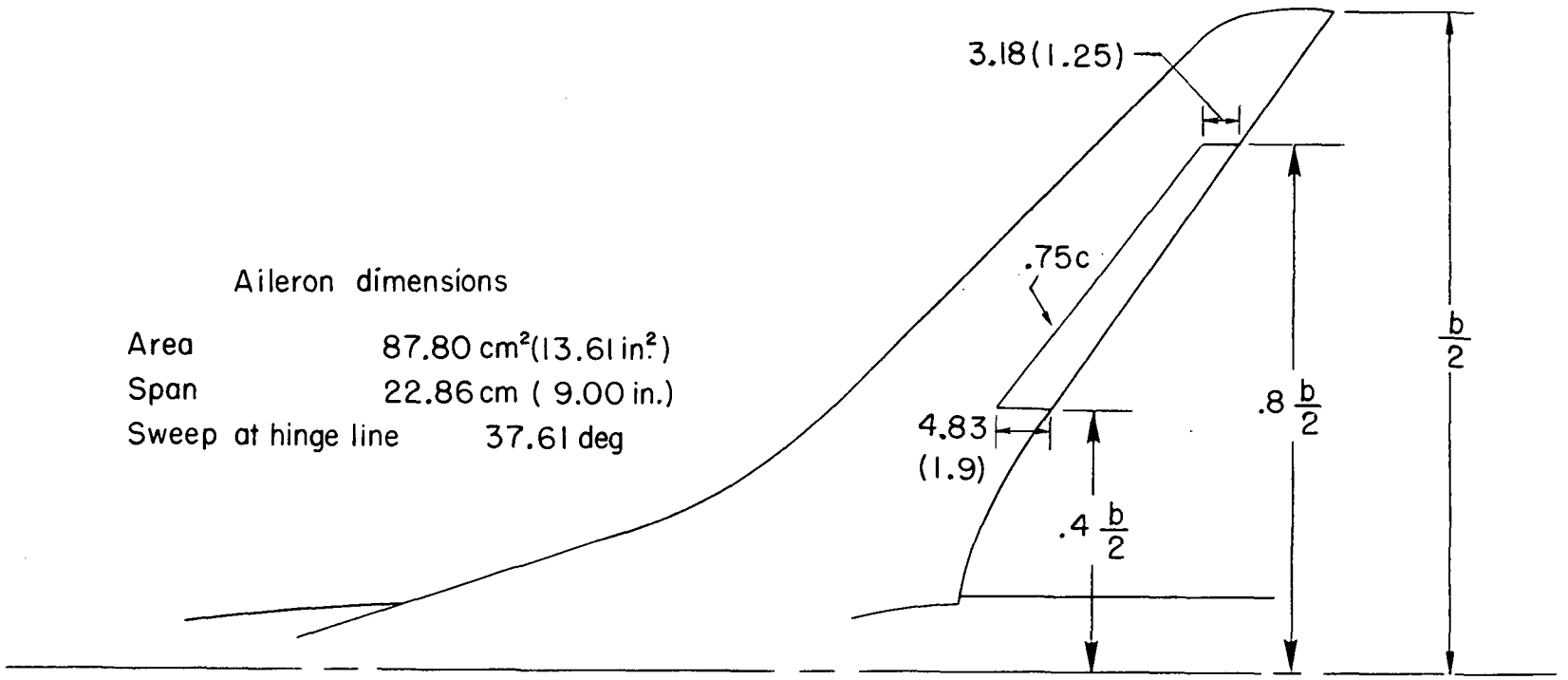

(b) Aileron geometry.

Figure 1.- Continued.

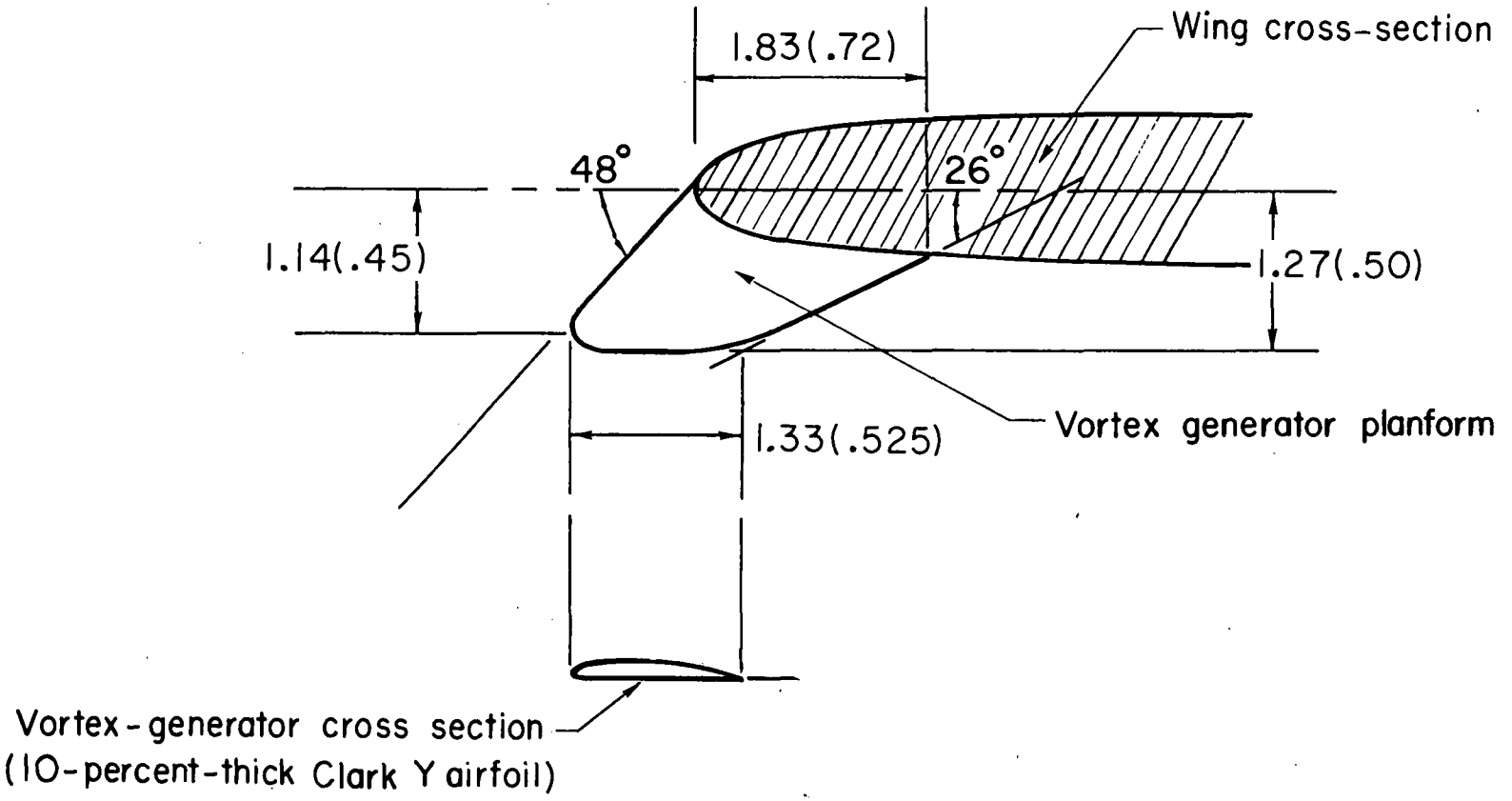

(c) Sketch of the underwing leading-edge vortex generator.

Figure 1.- Continued.

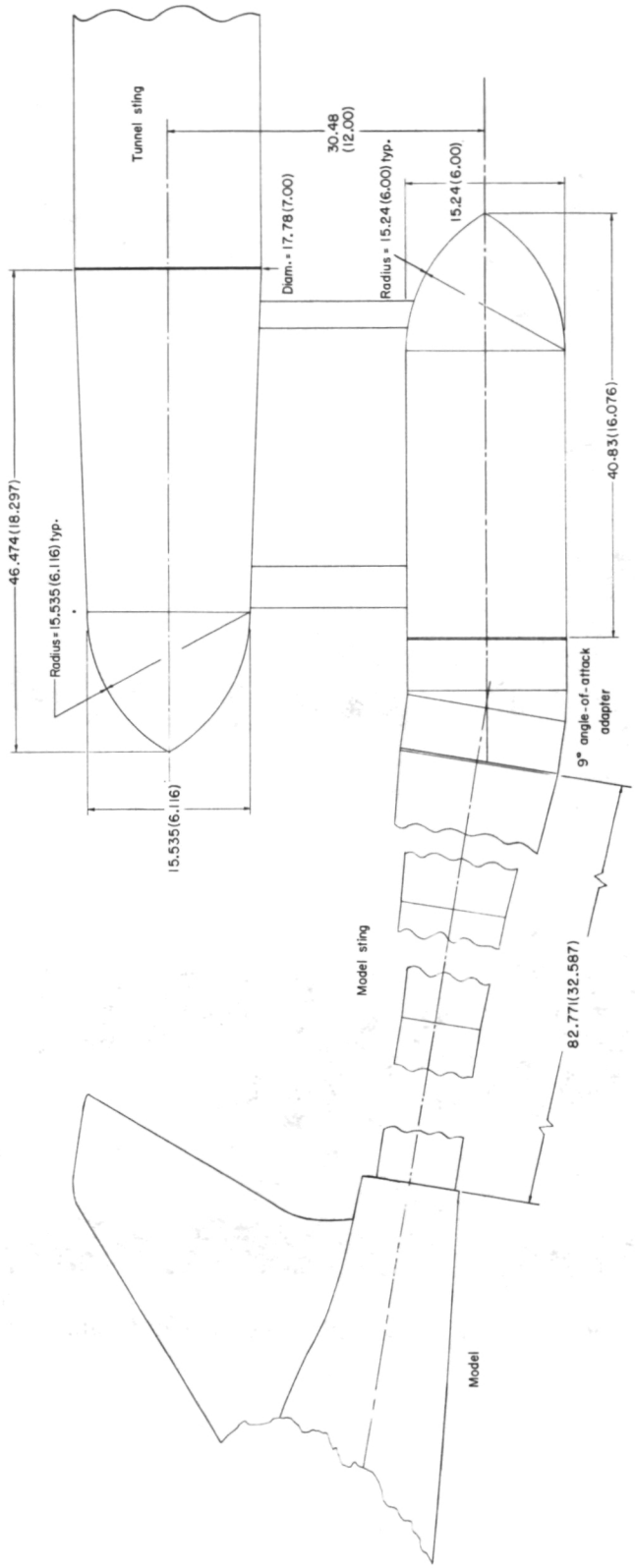

(d) Offset coupling sting arrangement.

Figure 1.- Concluded.

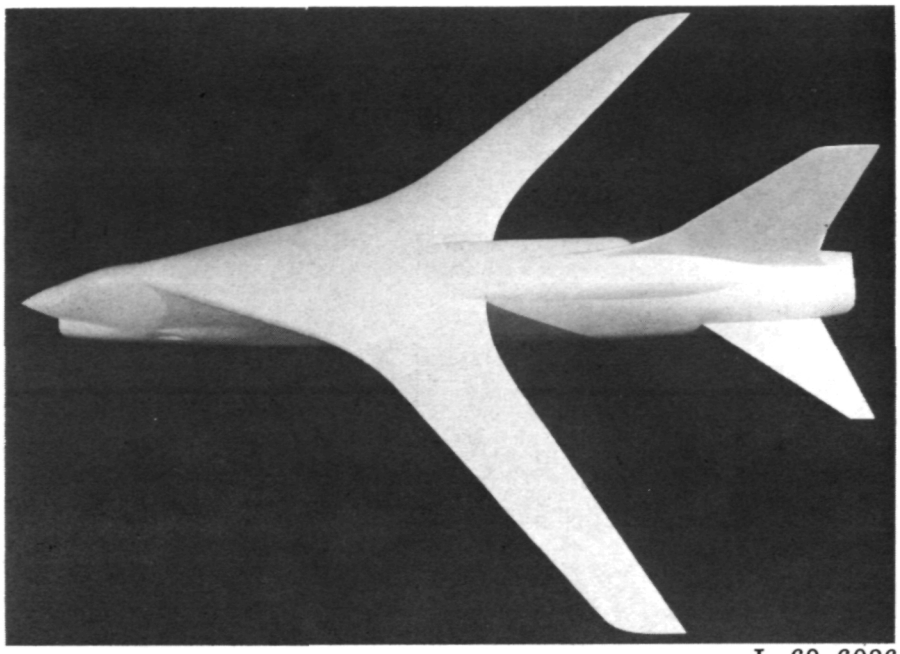

L-69-6086

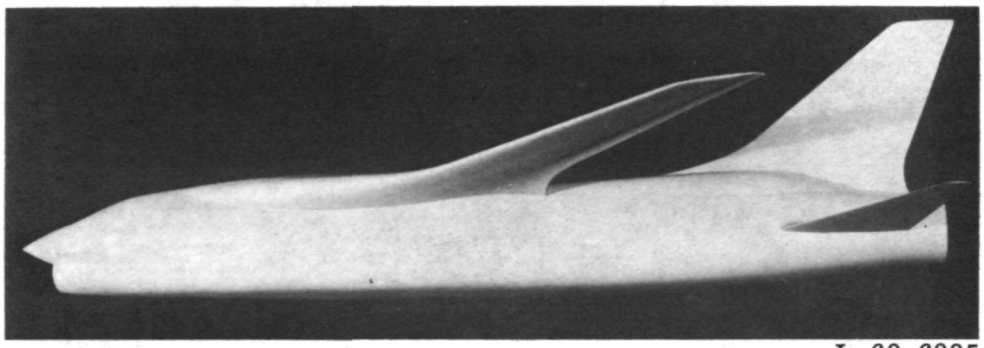

L-69-6085

Figure 2.- Photographs of the 0.087-scale wind-tunnel model.

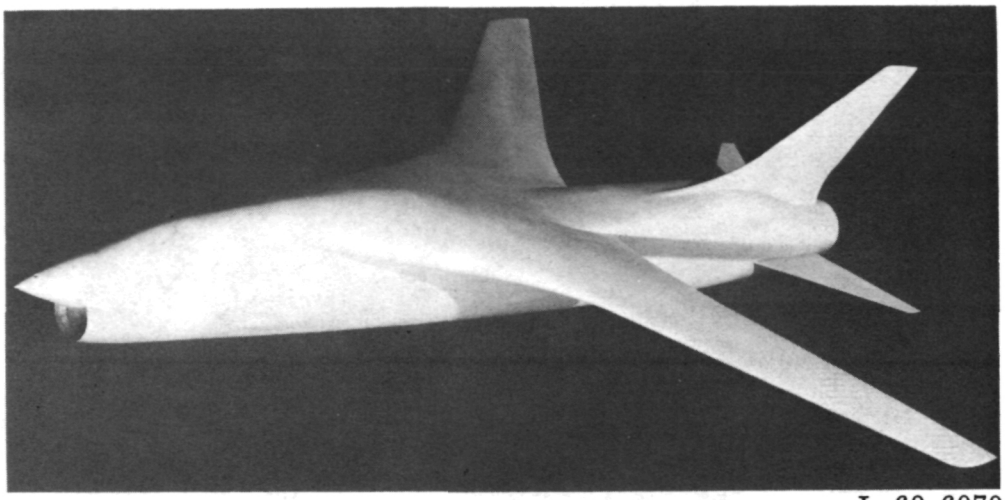

L-69-6079

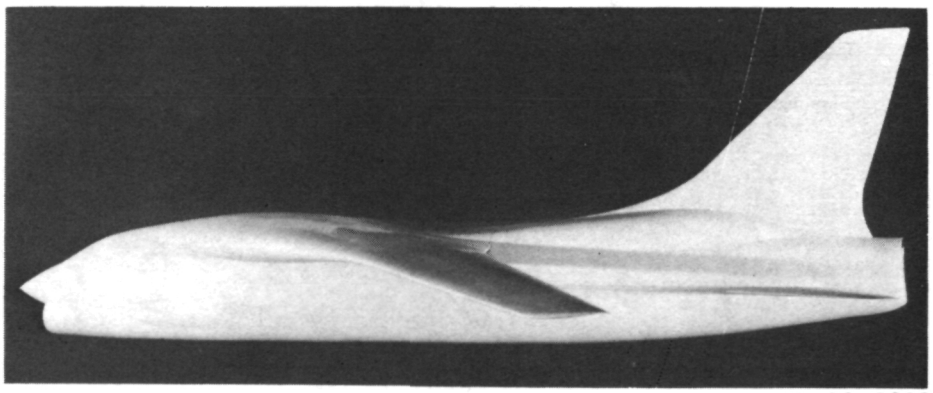

L-69-6083

Figure 2.- Concluded.

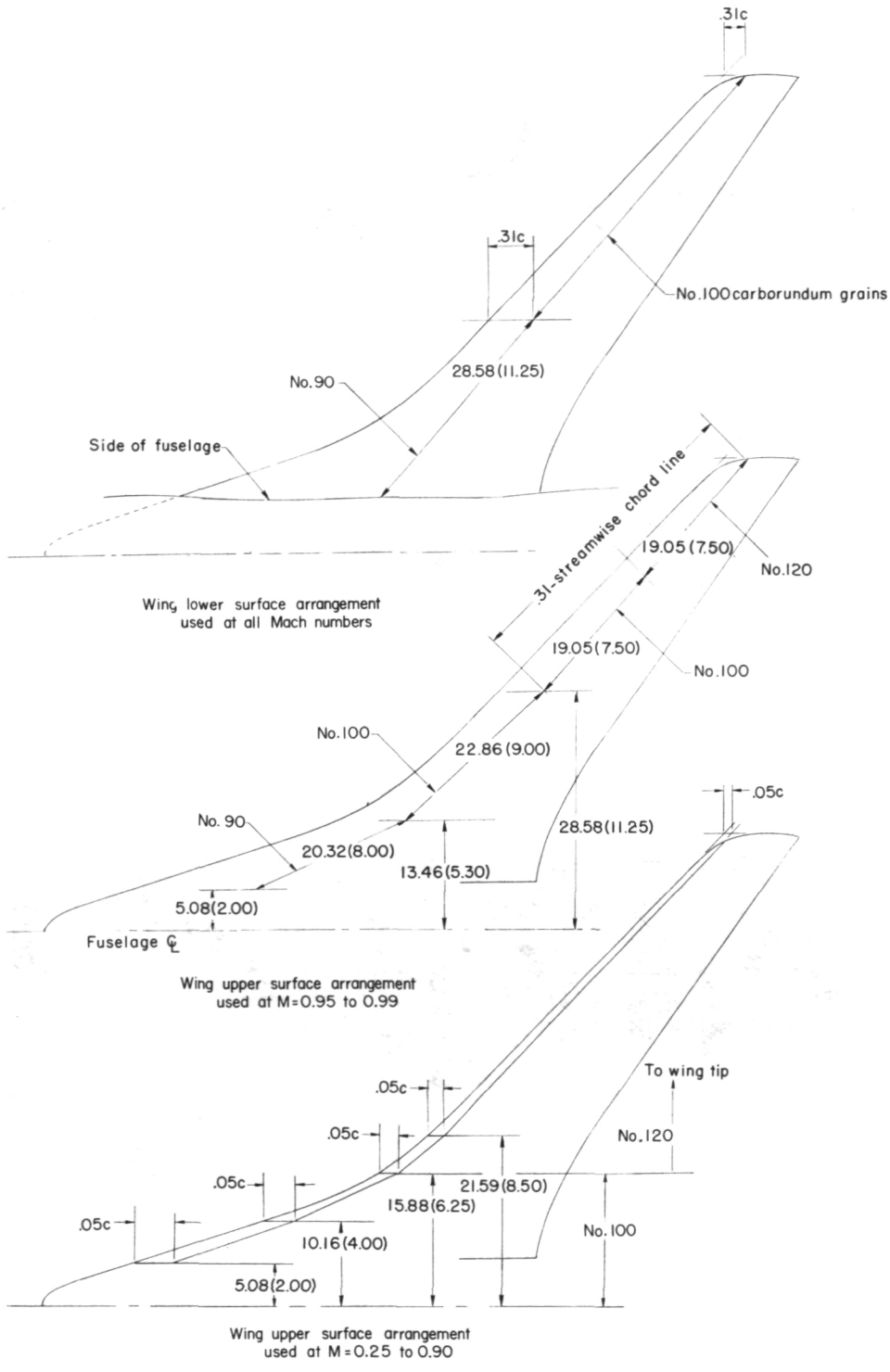

Figure 3.- Wing boundary-layer trip arrangements. Dimensions are in centimeters (inches).

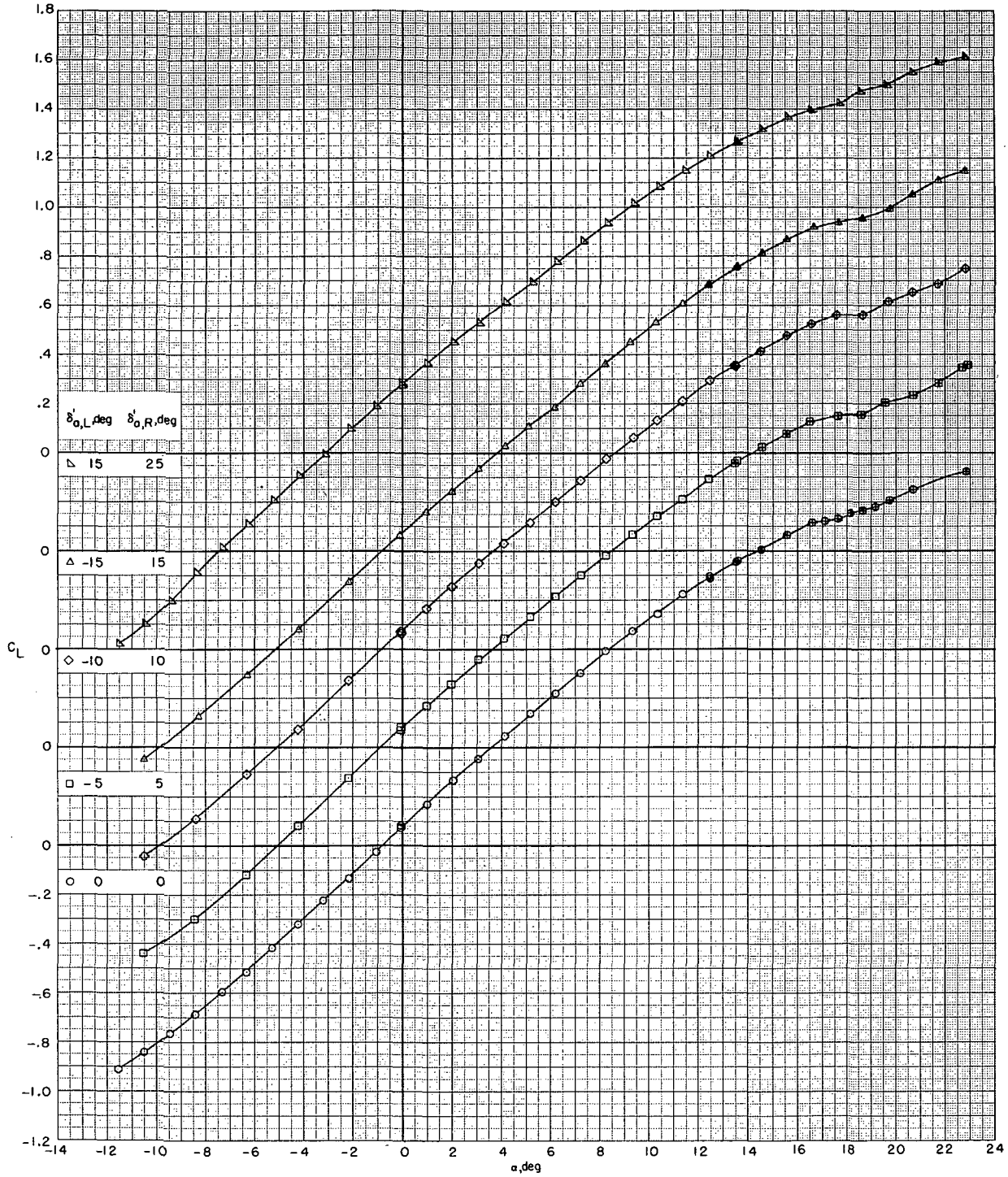

(a) M = 0.25.

Figure 4.- Effect of differential aileron deflection on the longitudinal aerodynamic coefficients $\delta_h = -2.5^o$.

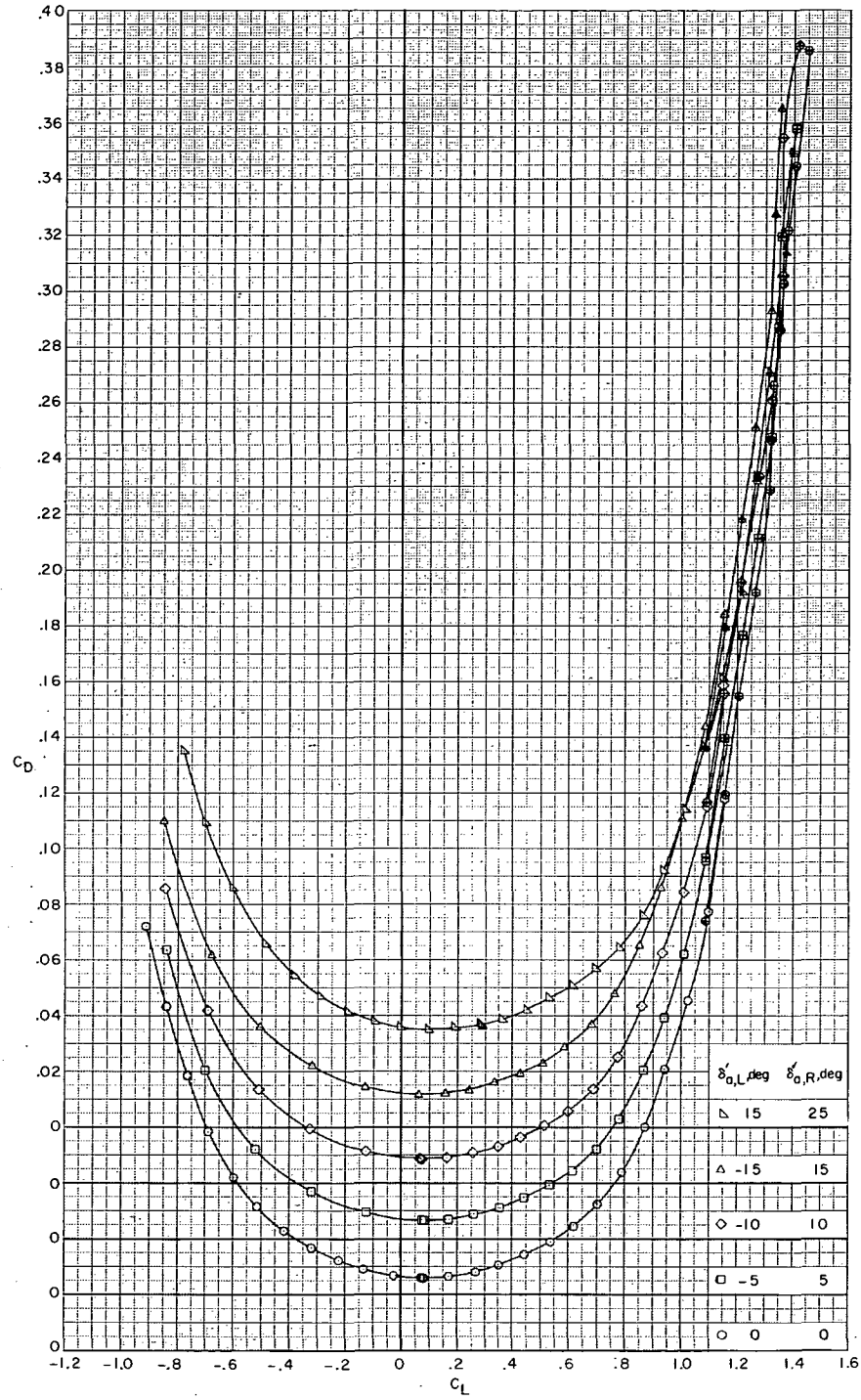

(a) M = 0.25. Continued.

Figure 4.- Continued.

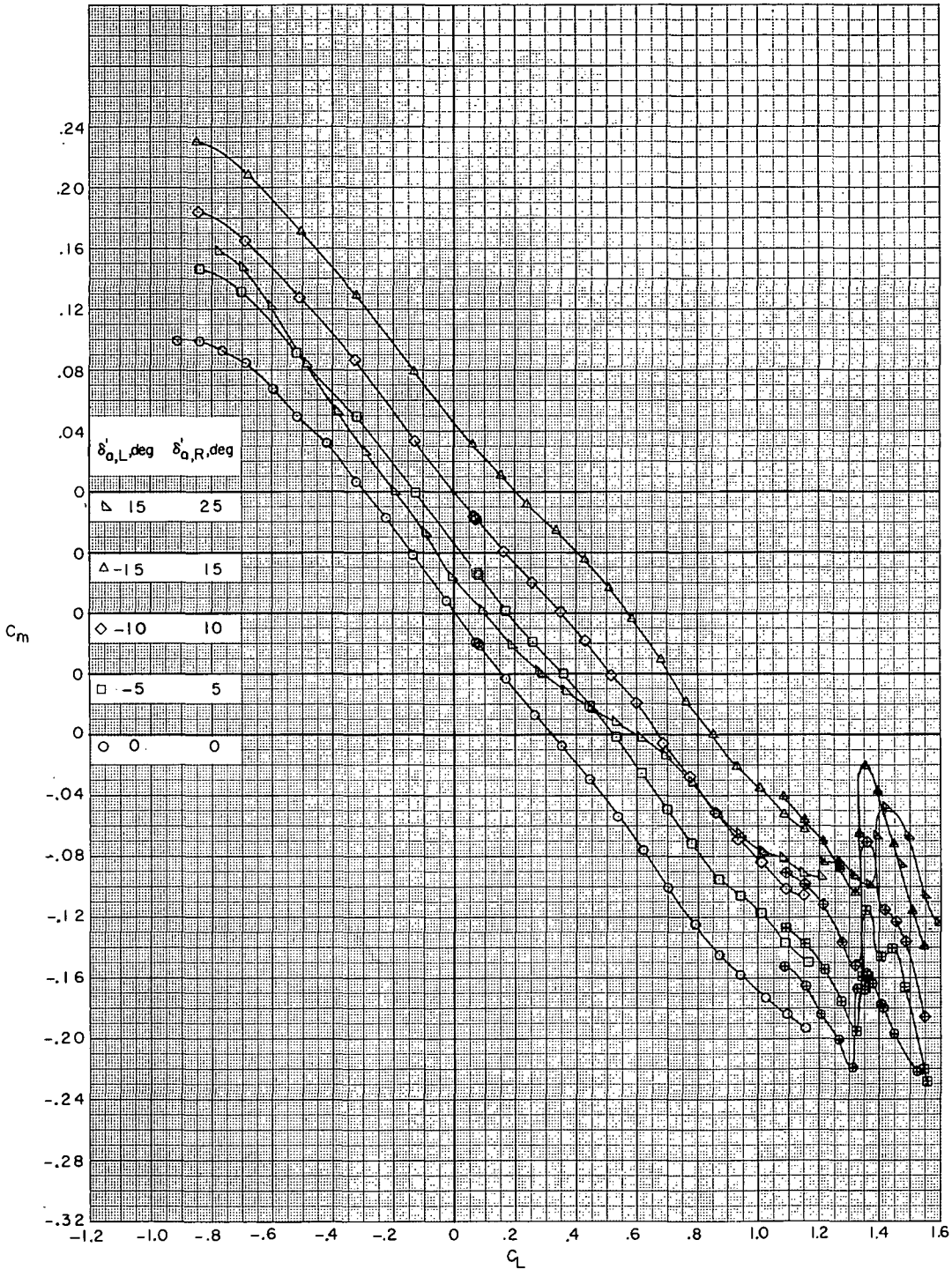

(a) M = 0.25. Concluded.

Figure 4.- Continued.

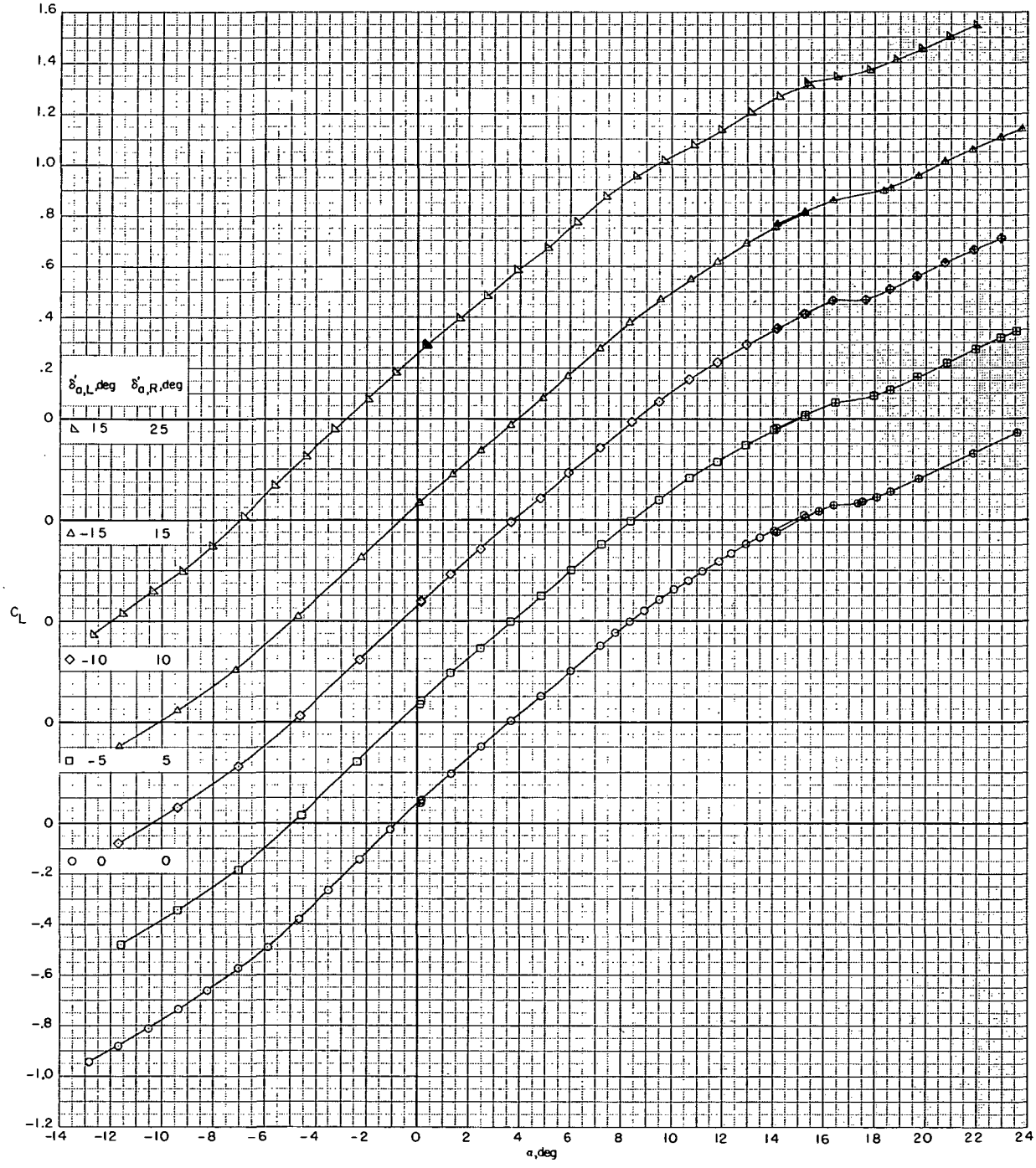

(b) M = 0.50.

Figure 4.- Continued.

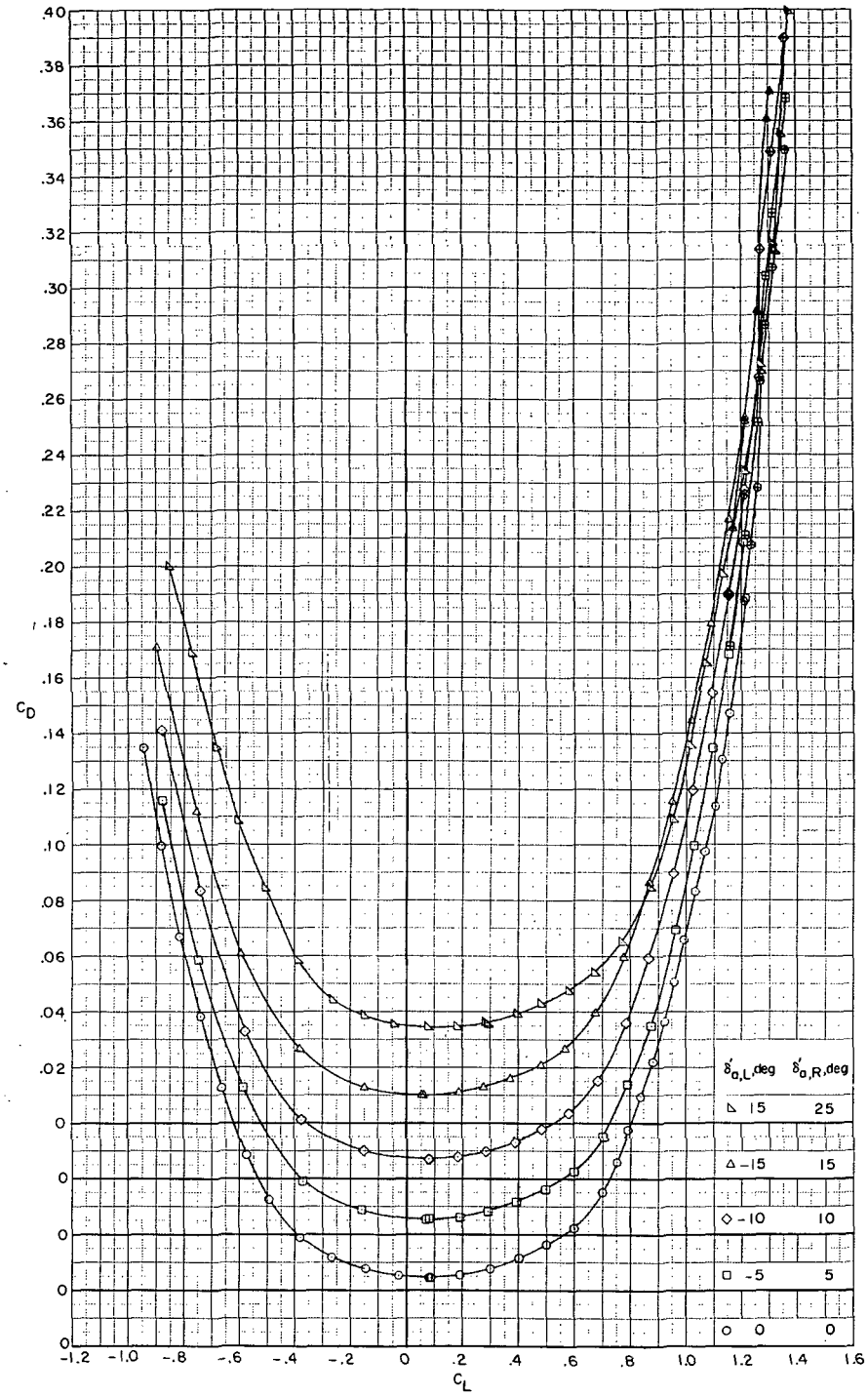

(b) M = 0.50. Continued.

Figure 4.- Continued.

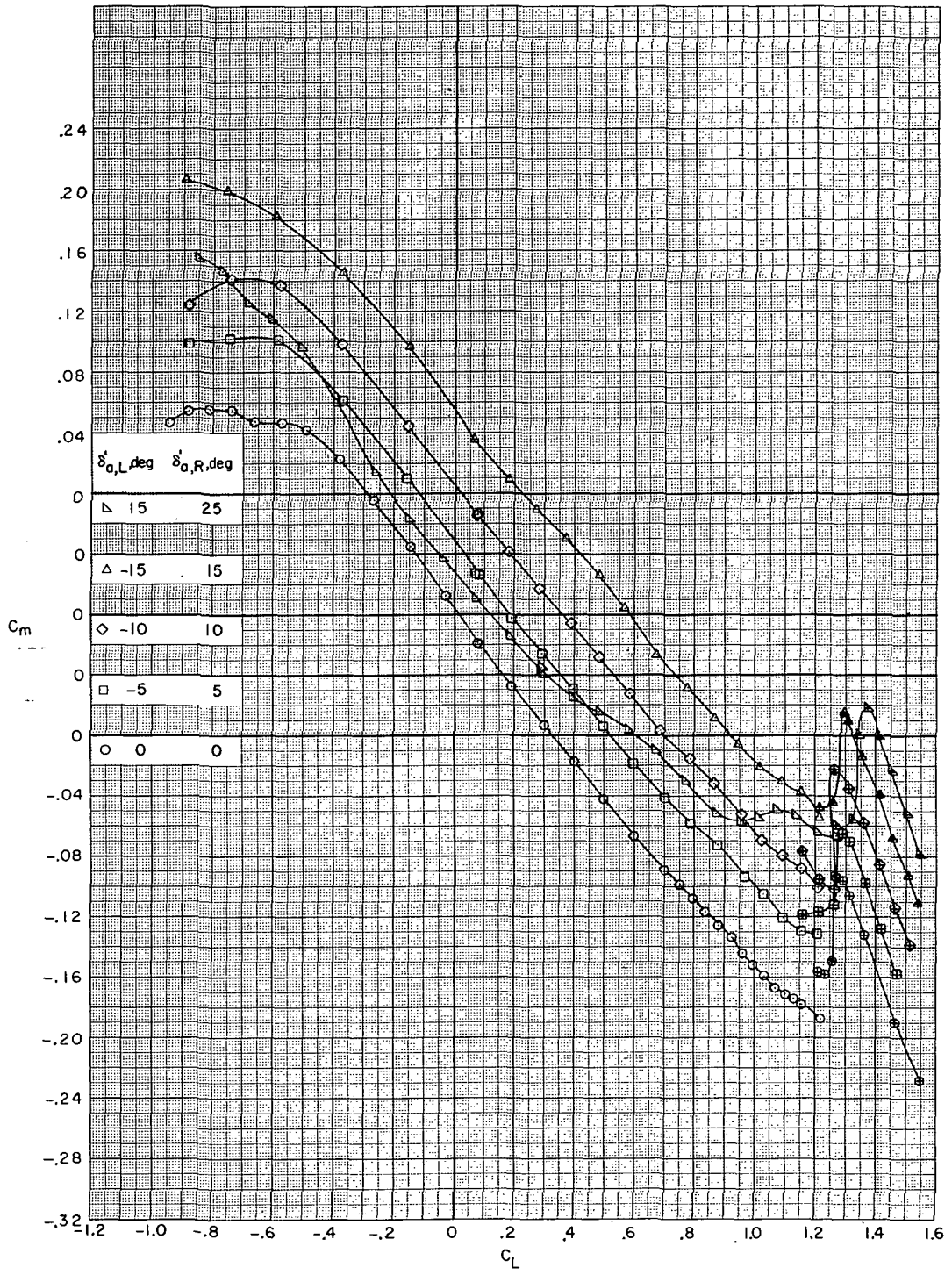

(b) M = 0.50. Concluded.

Figure 4.- Continued.

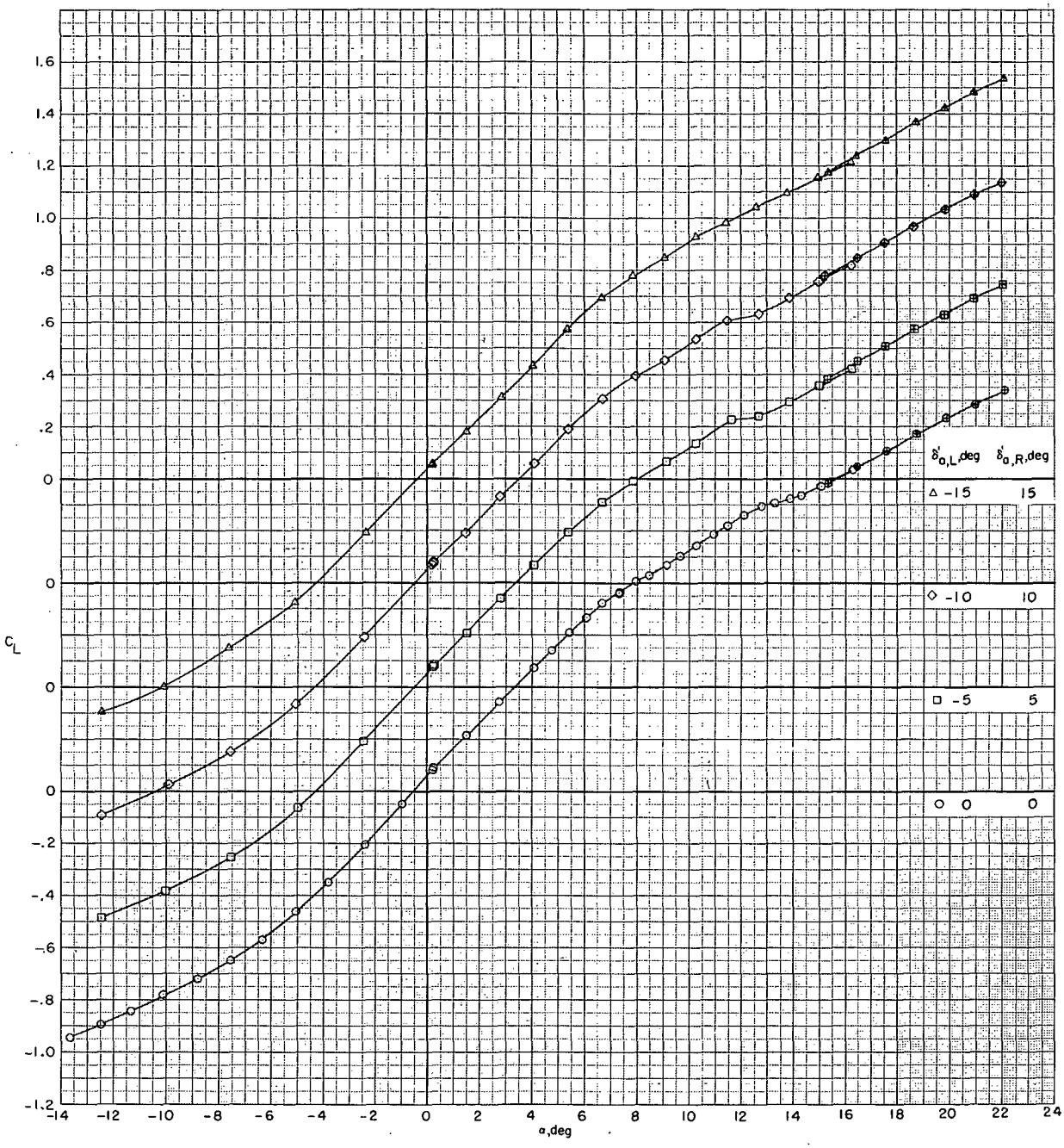

(c) M = 0.80.

Figure 4.- Continued.

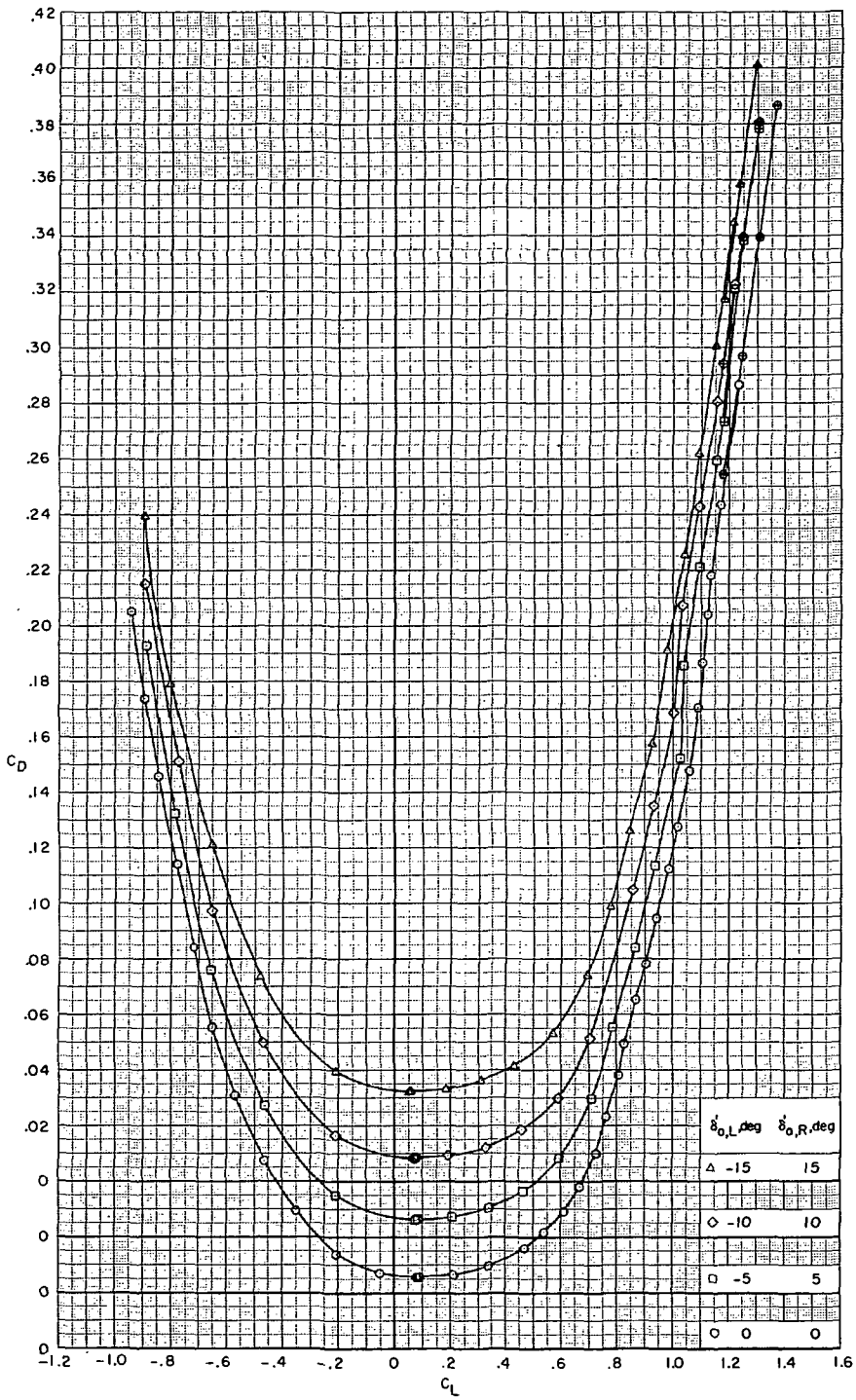

(c) M = 0.80. Continued.

Figure 4.- Continued.

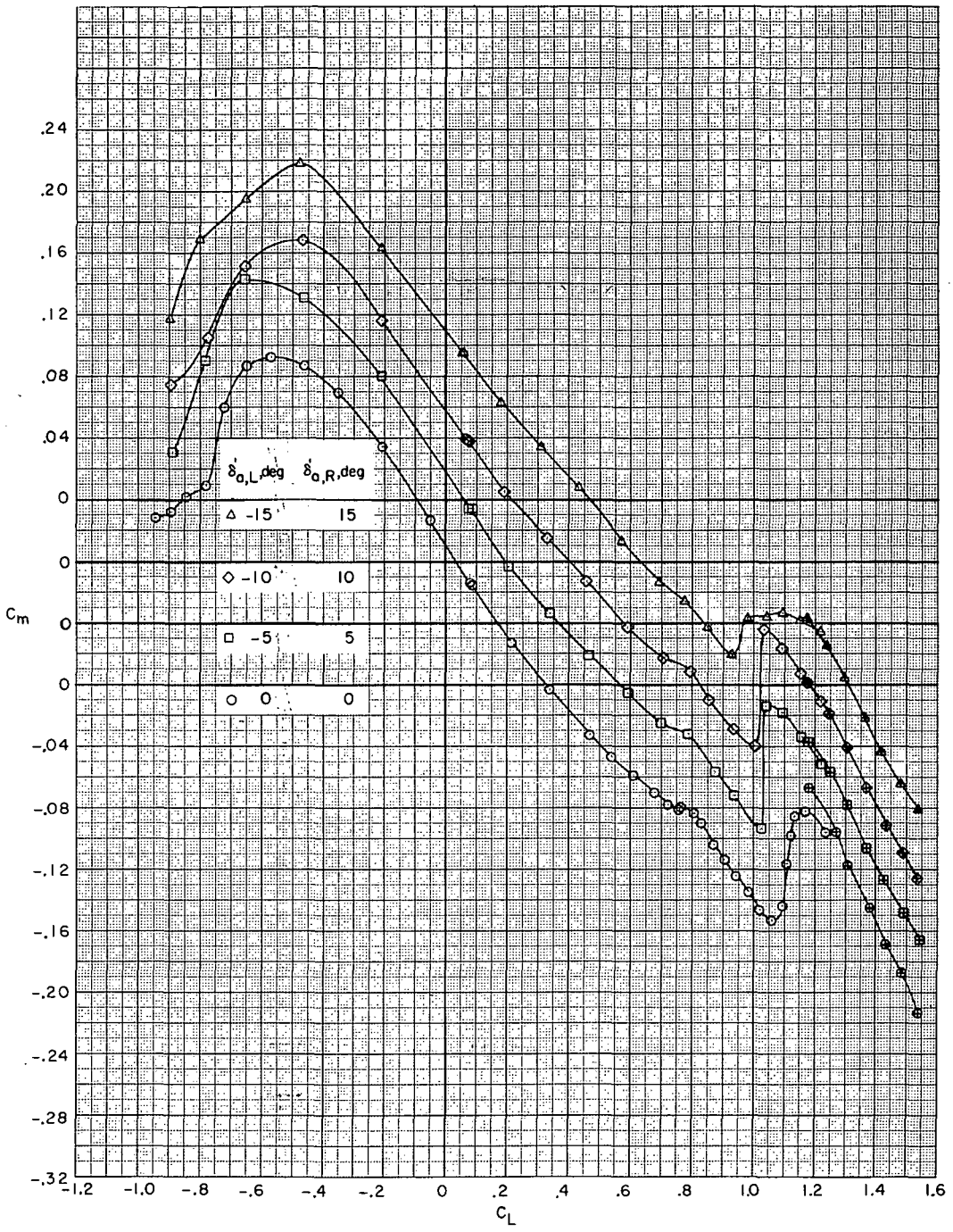

(c) M = 0.80. Concluded.

Figure 4.- Continued.

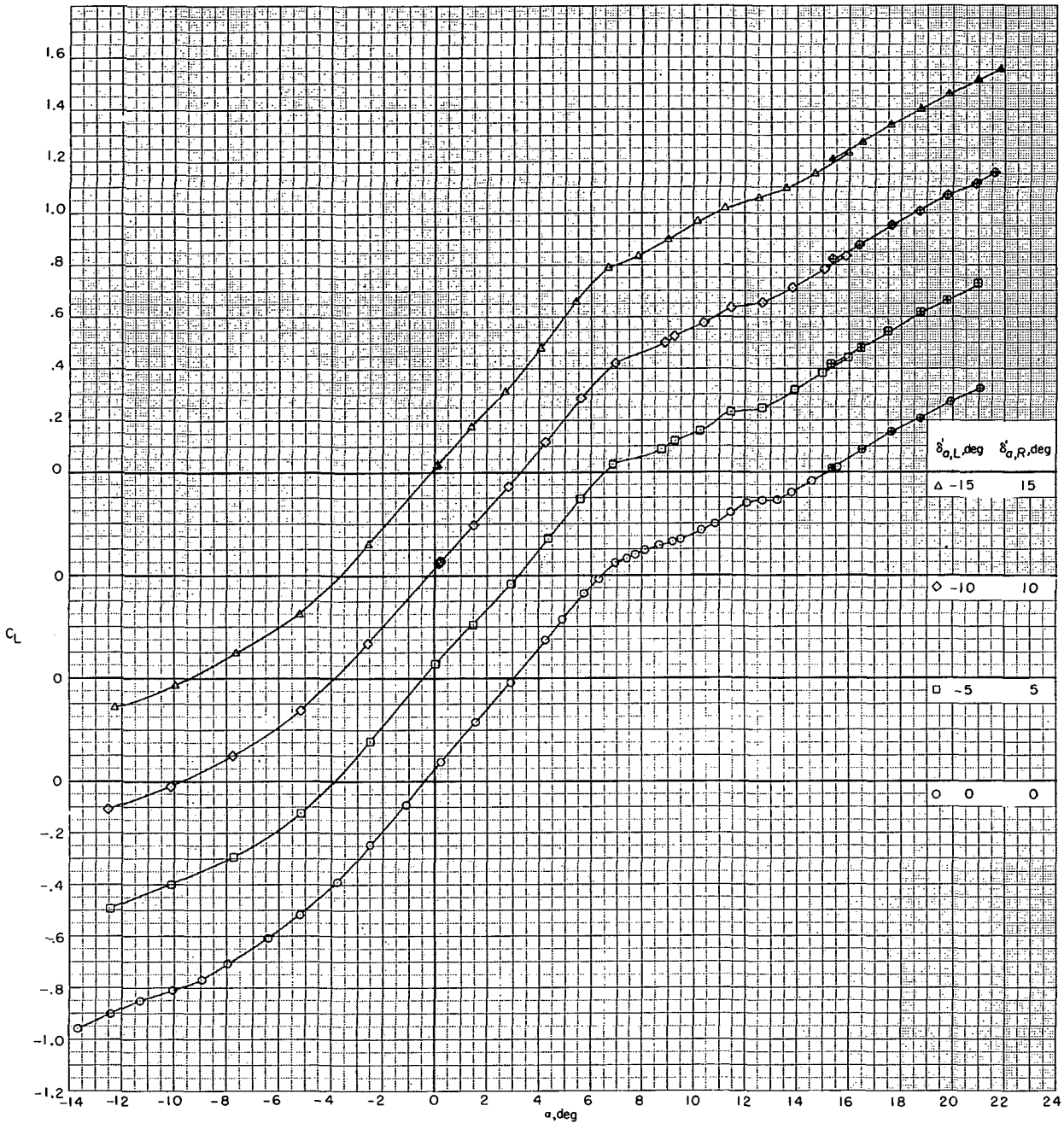

(d) M = 0.90.

Figure 4.- Continued.

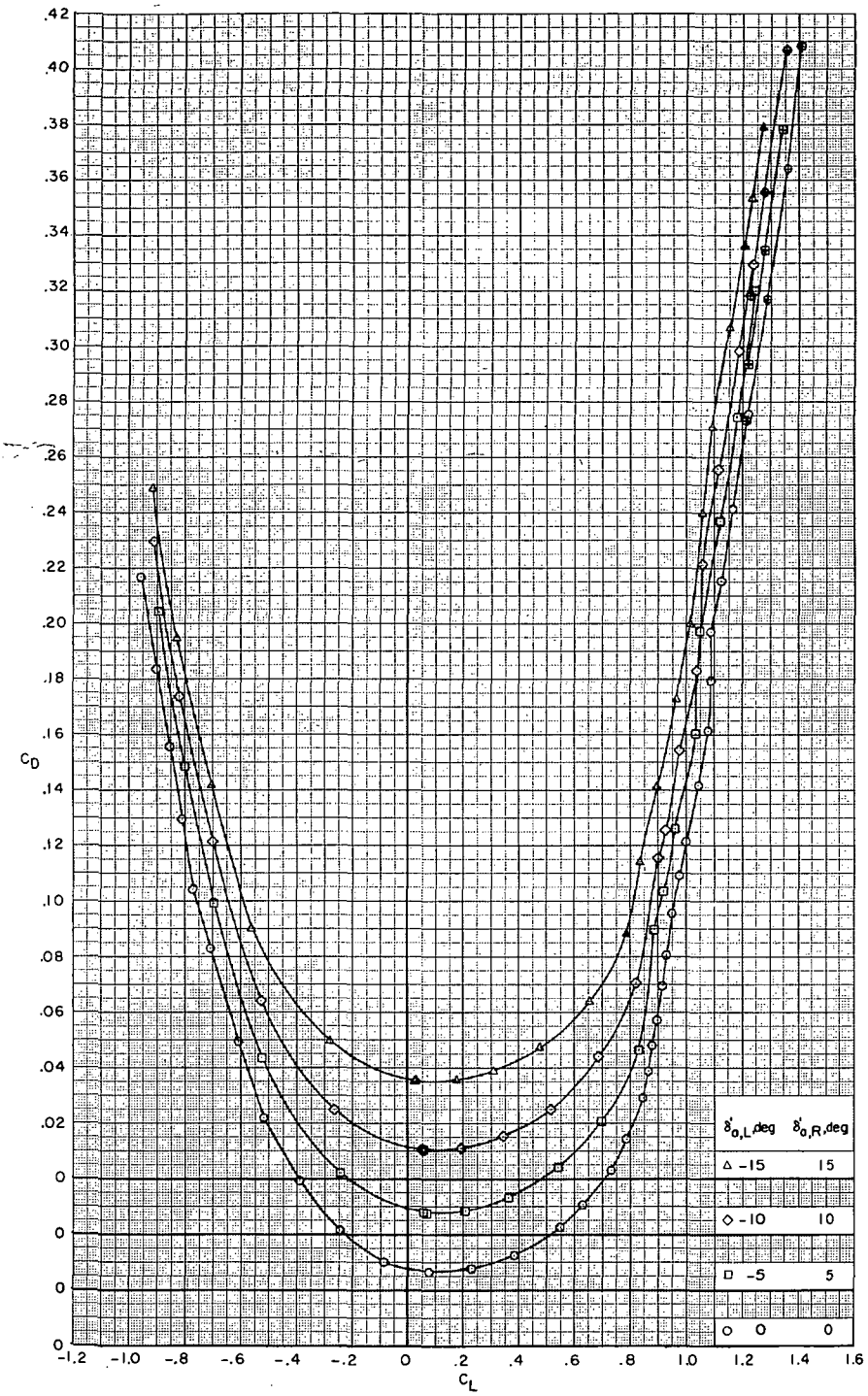

(d) M = 0.90. Continued.

Figure 4.- Continued.

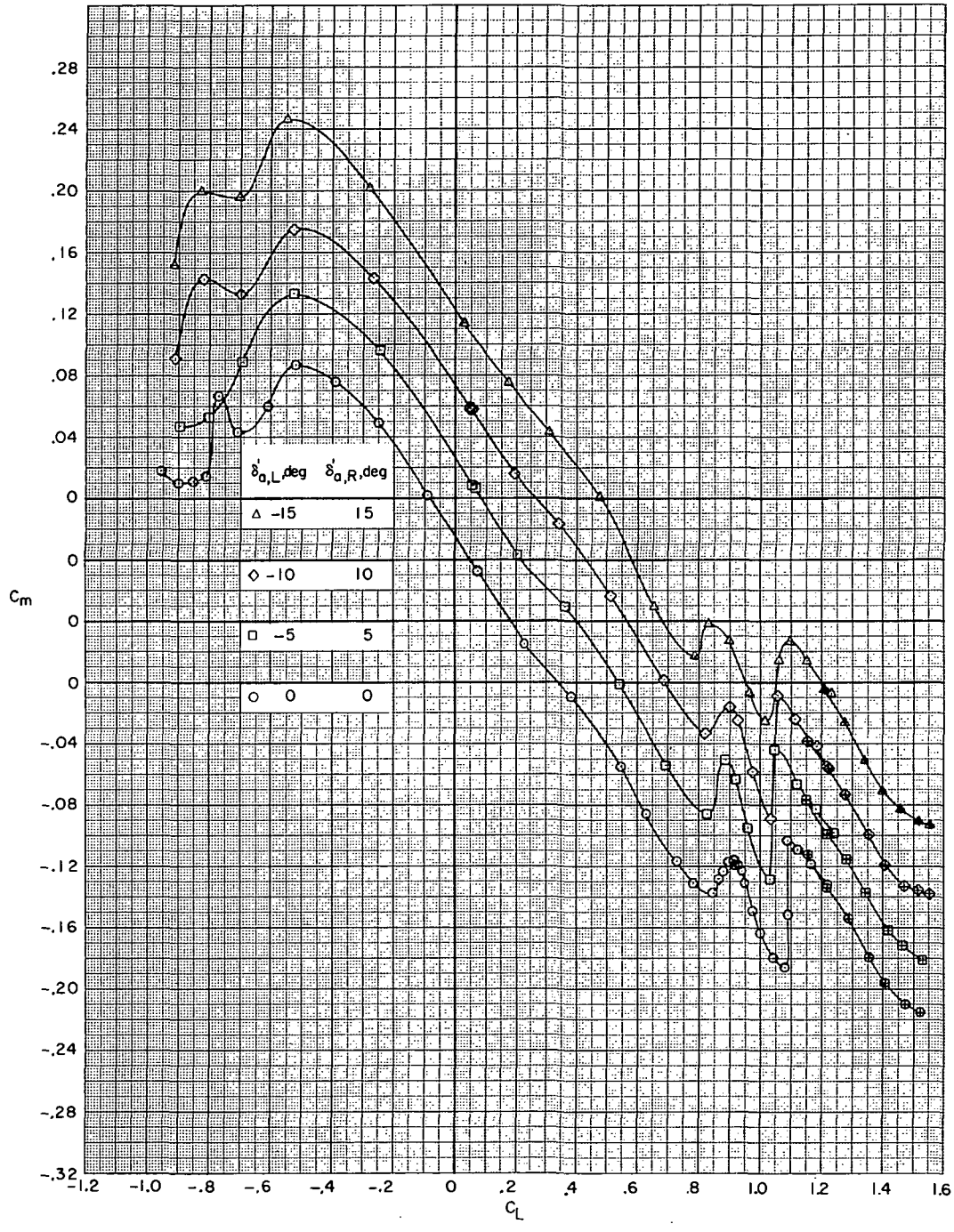

(d) M = 0.90. Concluded.

Figure 4.- Continued.

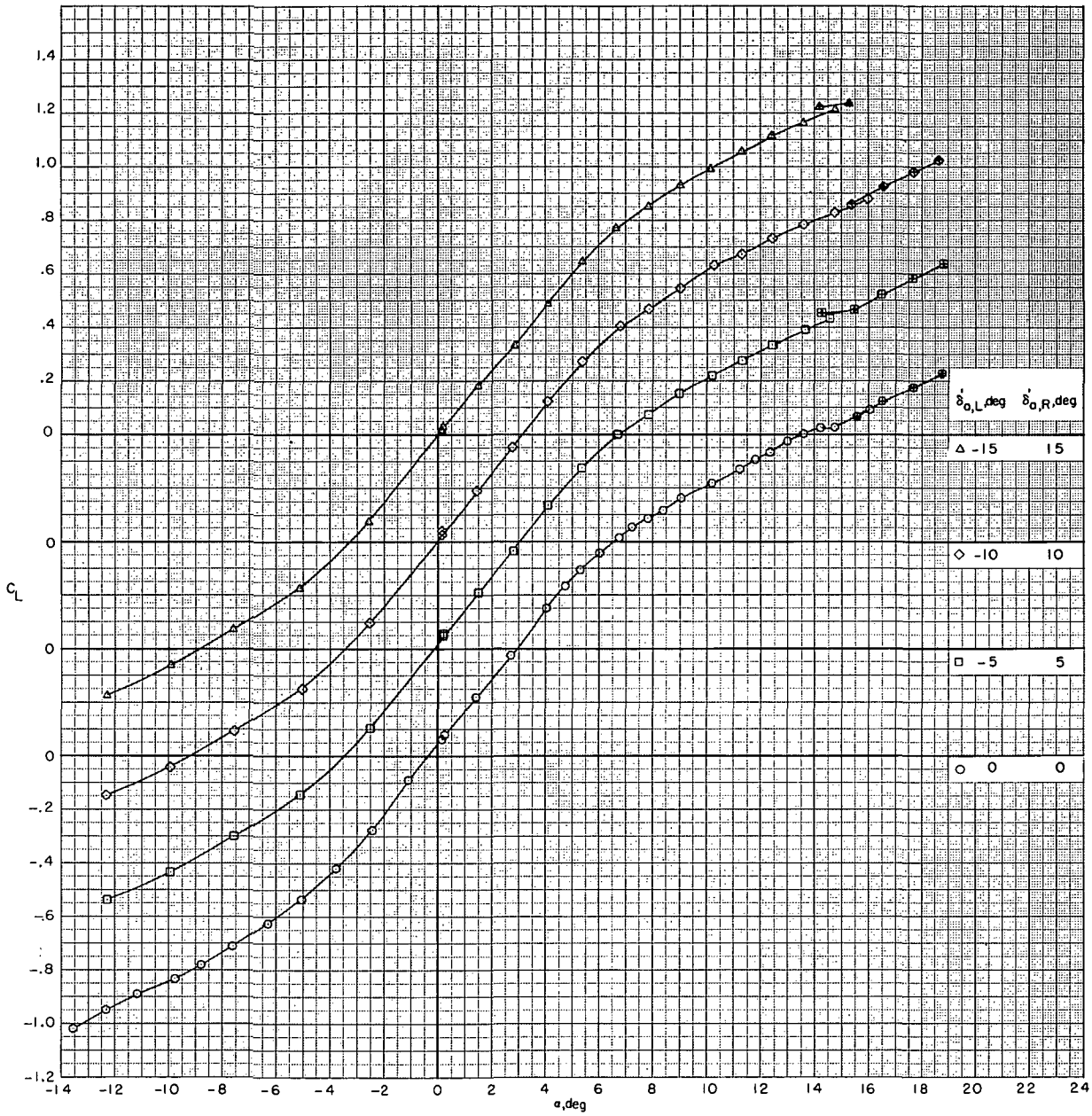

(e) M = 0.95.

Figure 4.- Continued.

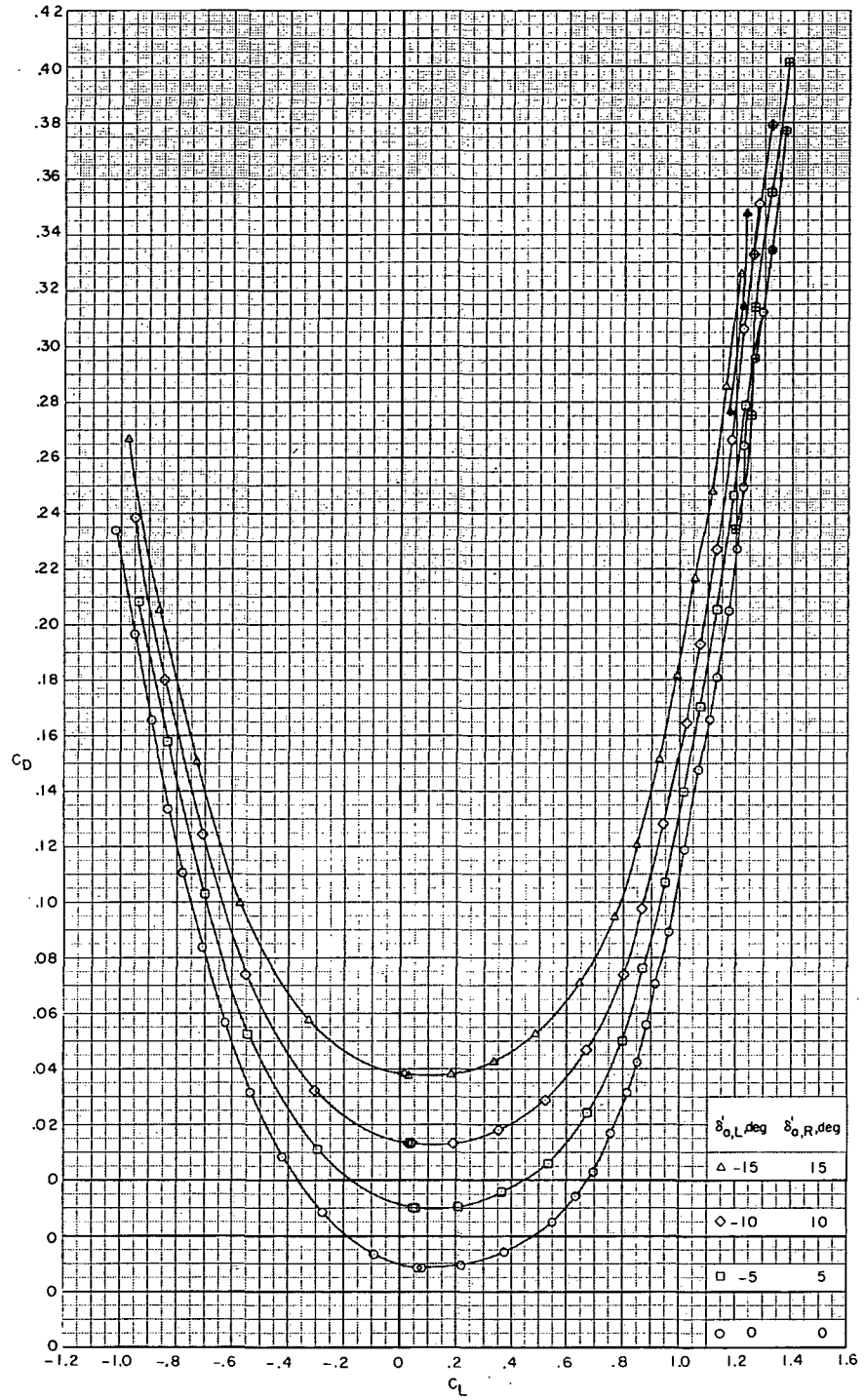

(e) M = 0.95. Continued.

Figure 4.- Continued.

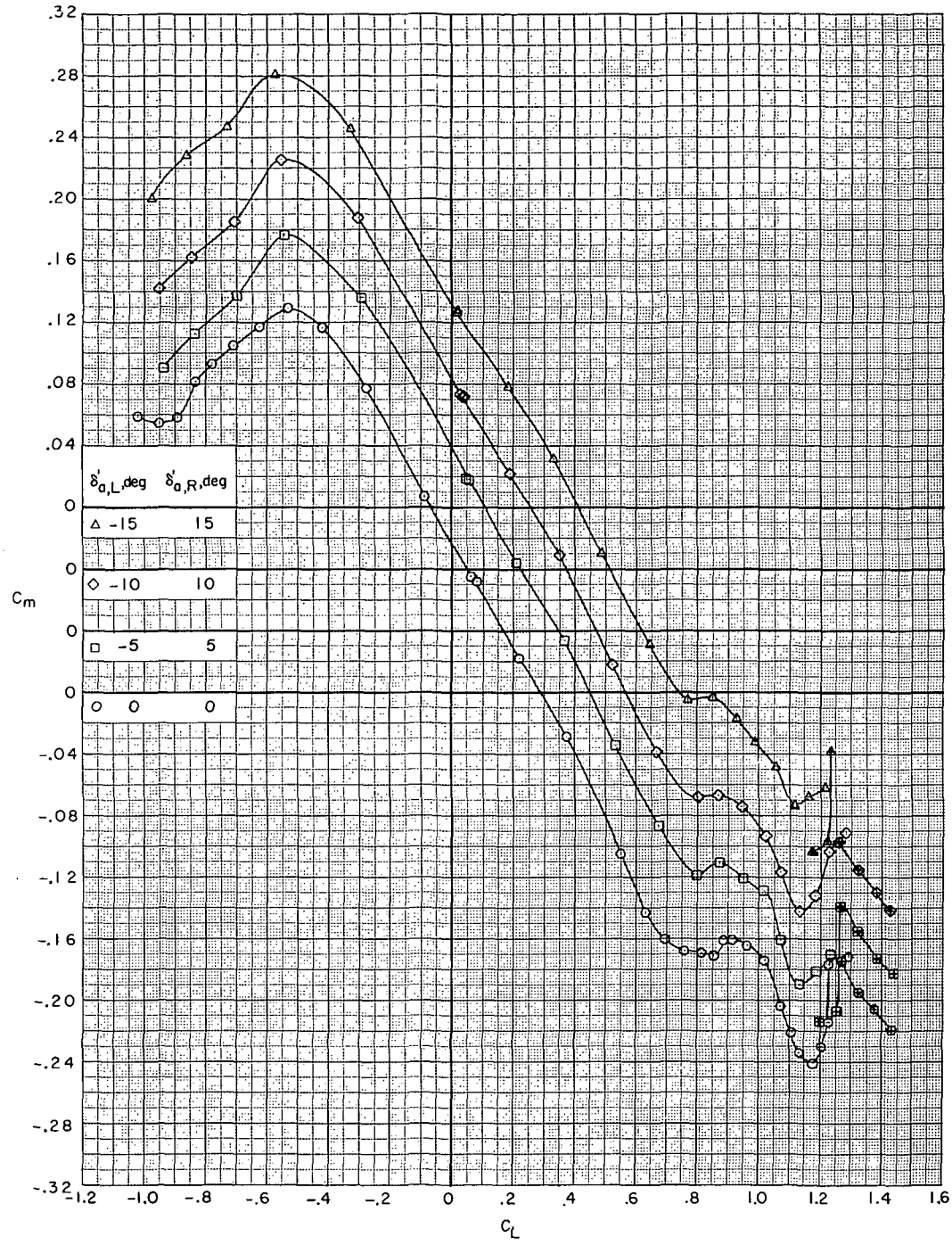

(e) M = 0.95. Concluded.

Figure 4.- Continued.

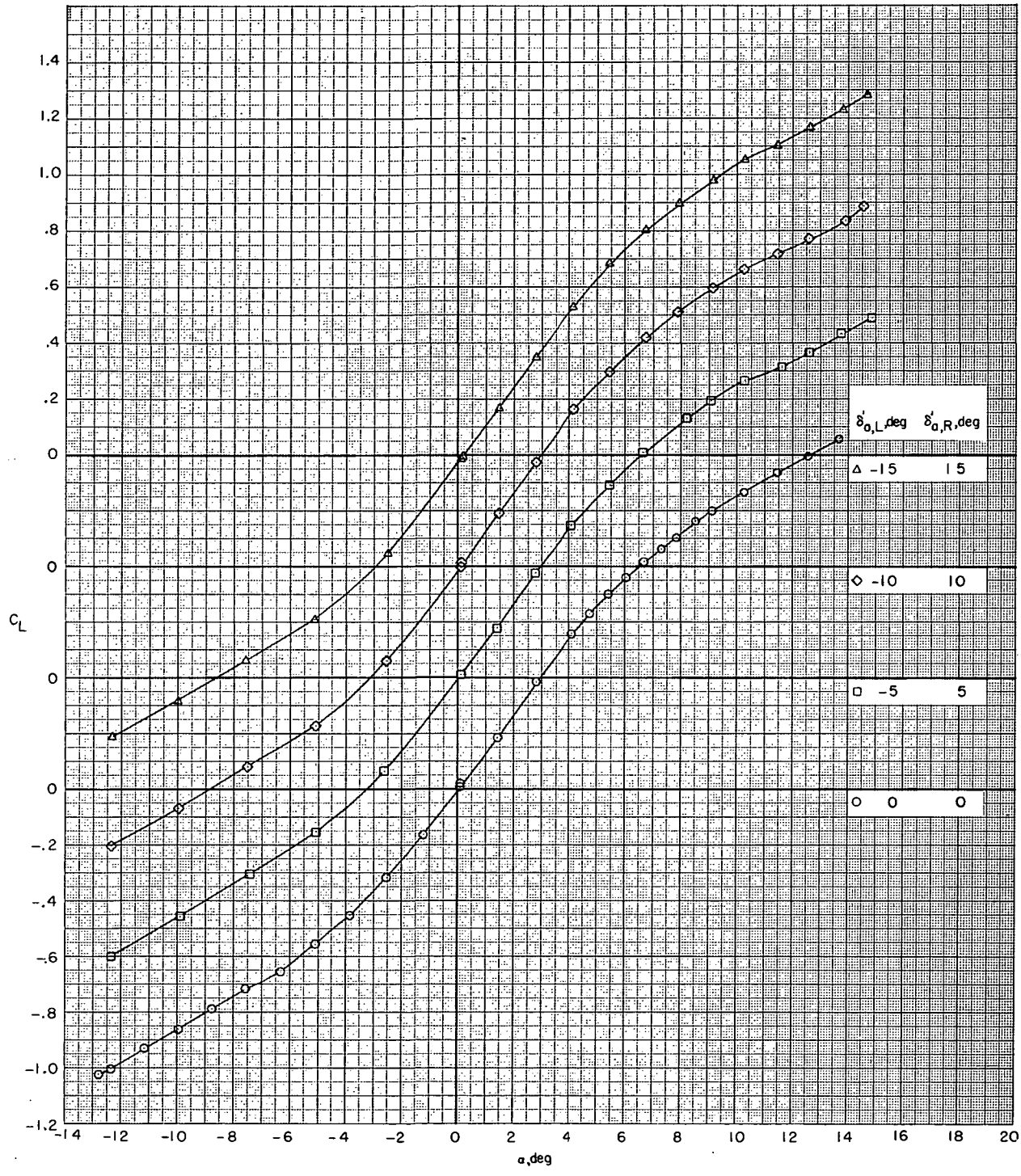

(f) M = 0.99.

Figure 4.- Continued.

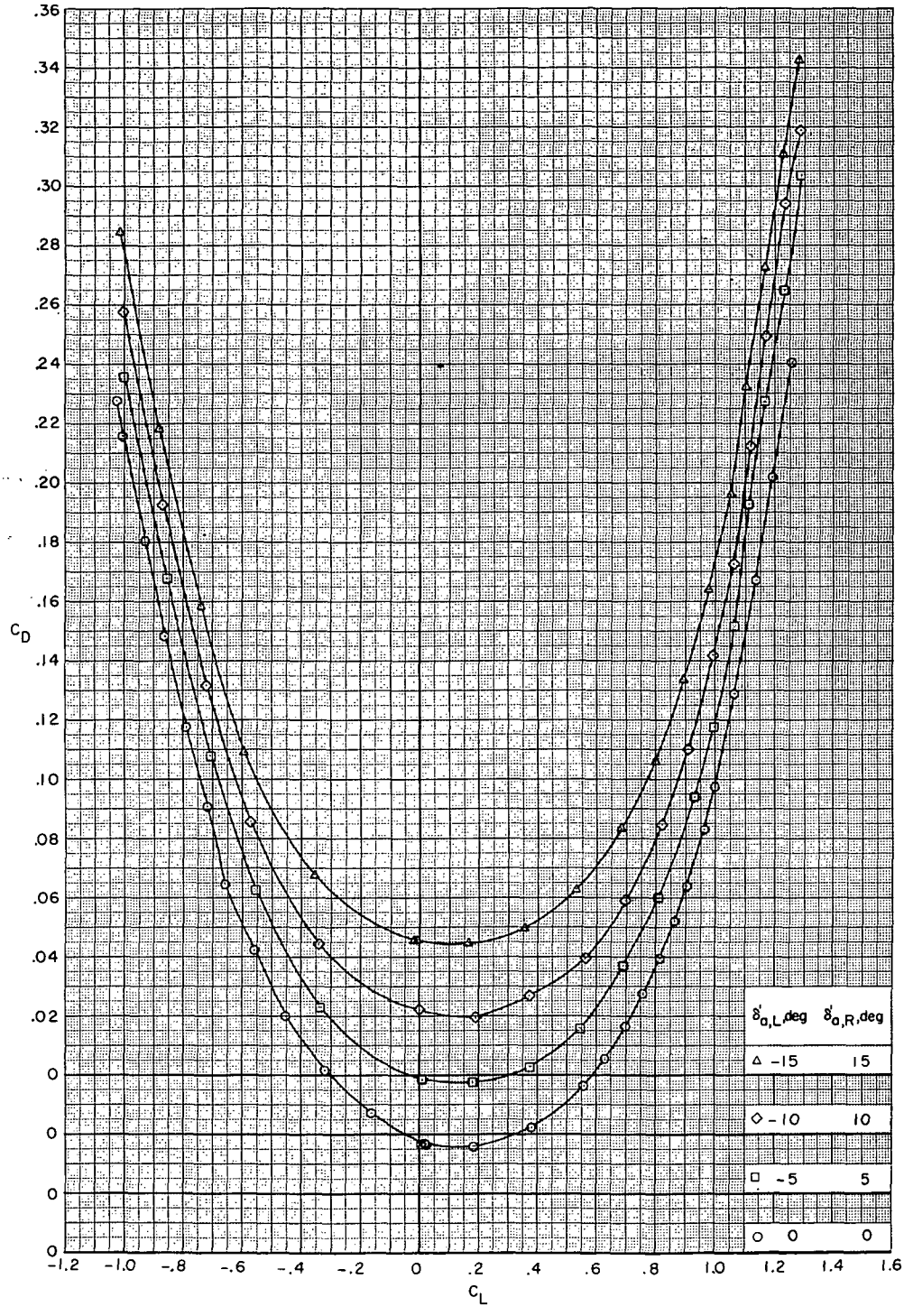

(f) M = 0.99. Continued.

Figure 4.- Continued.

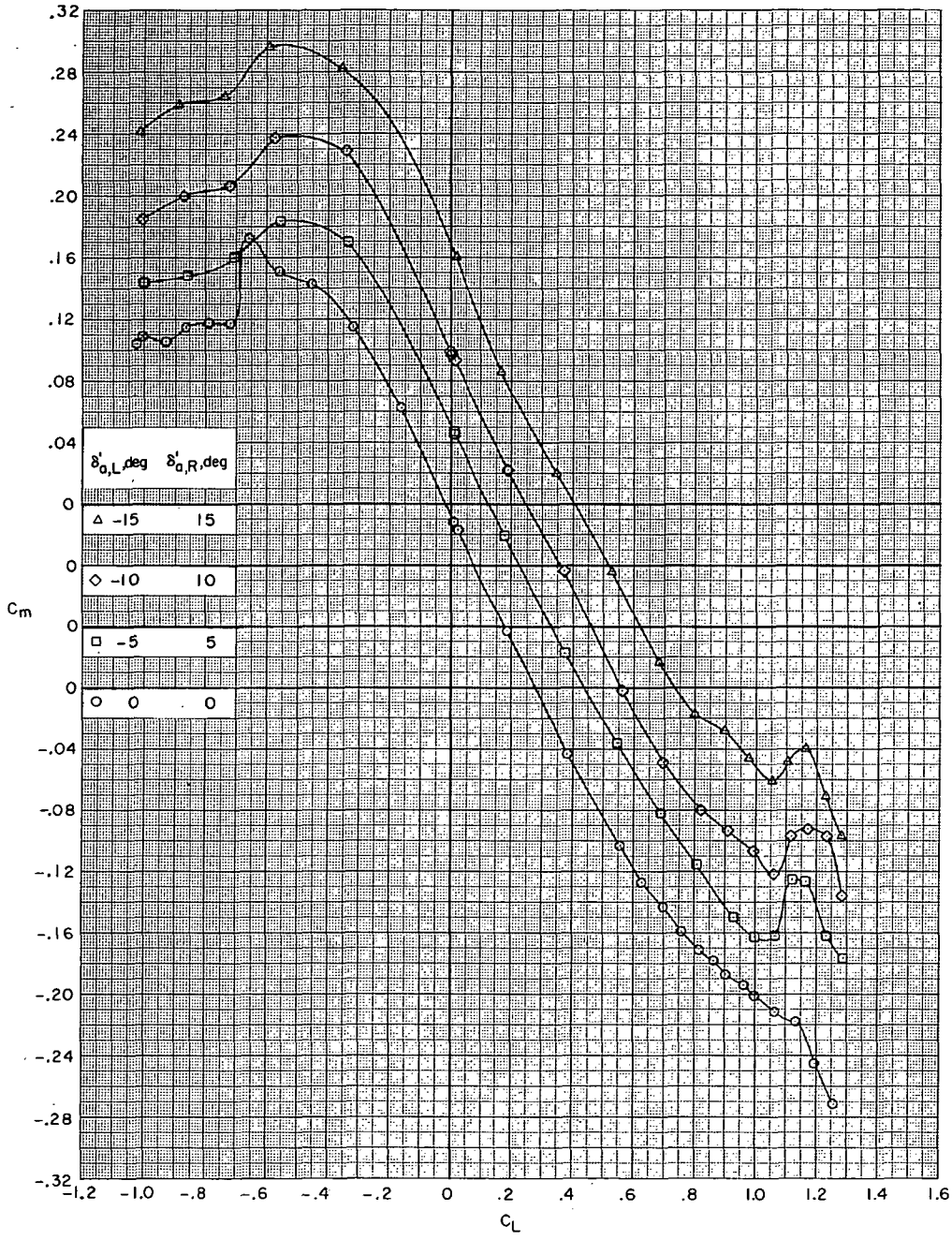

(f) M = 0.99. Concluded.

Figure 4.- Concluded.

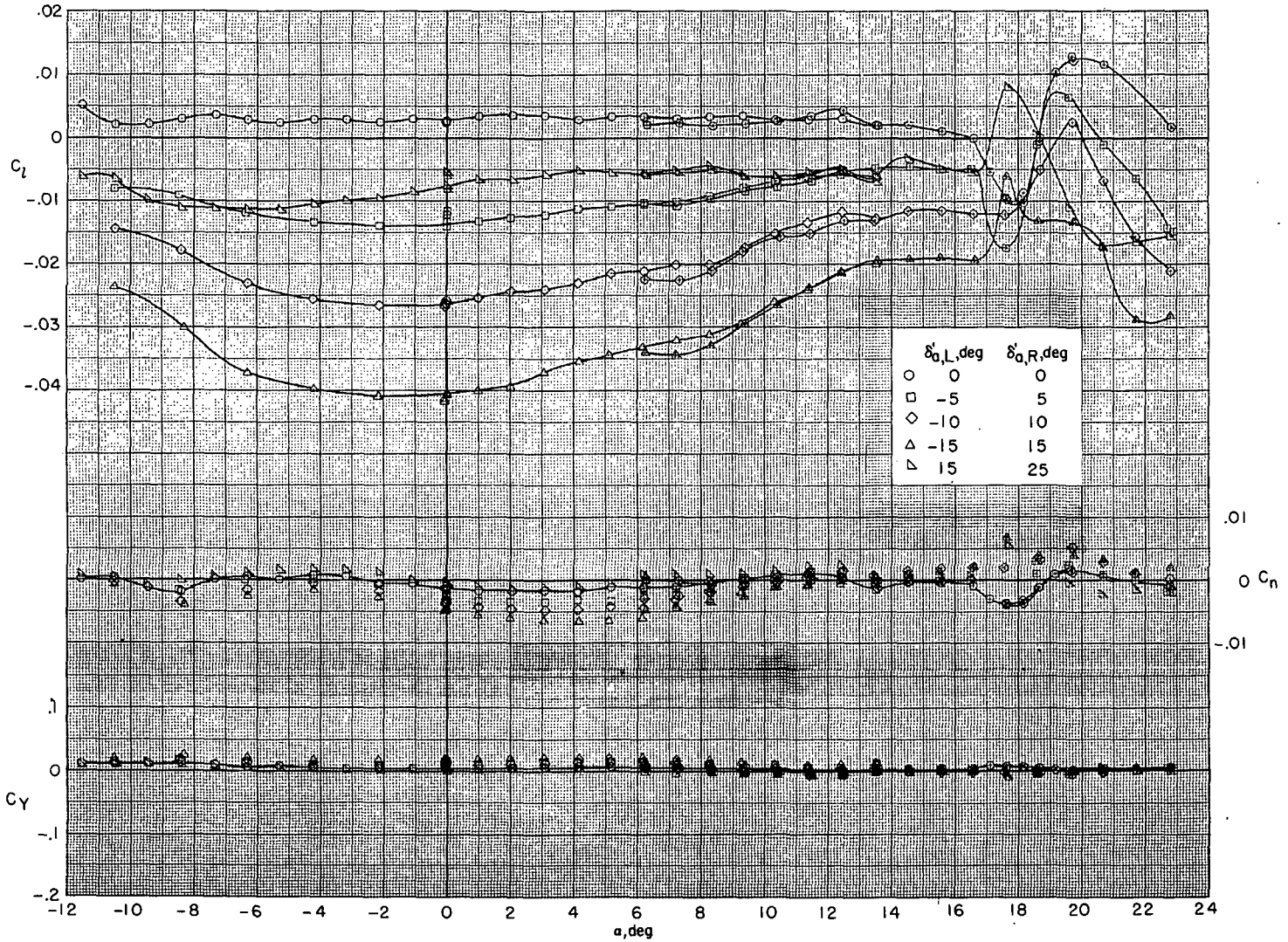

(a) M = 0.25.

Figure 5.- Effect of differential aileron deflection on the lateral-directional aerodynamic coefficients. $\delta_h = -2.5^o$.

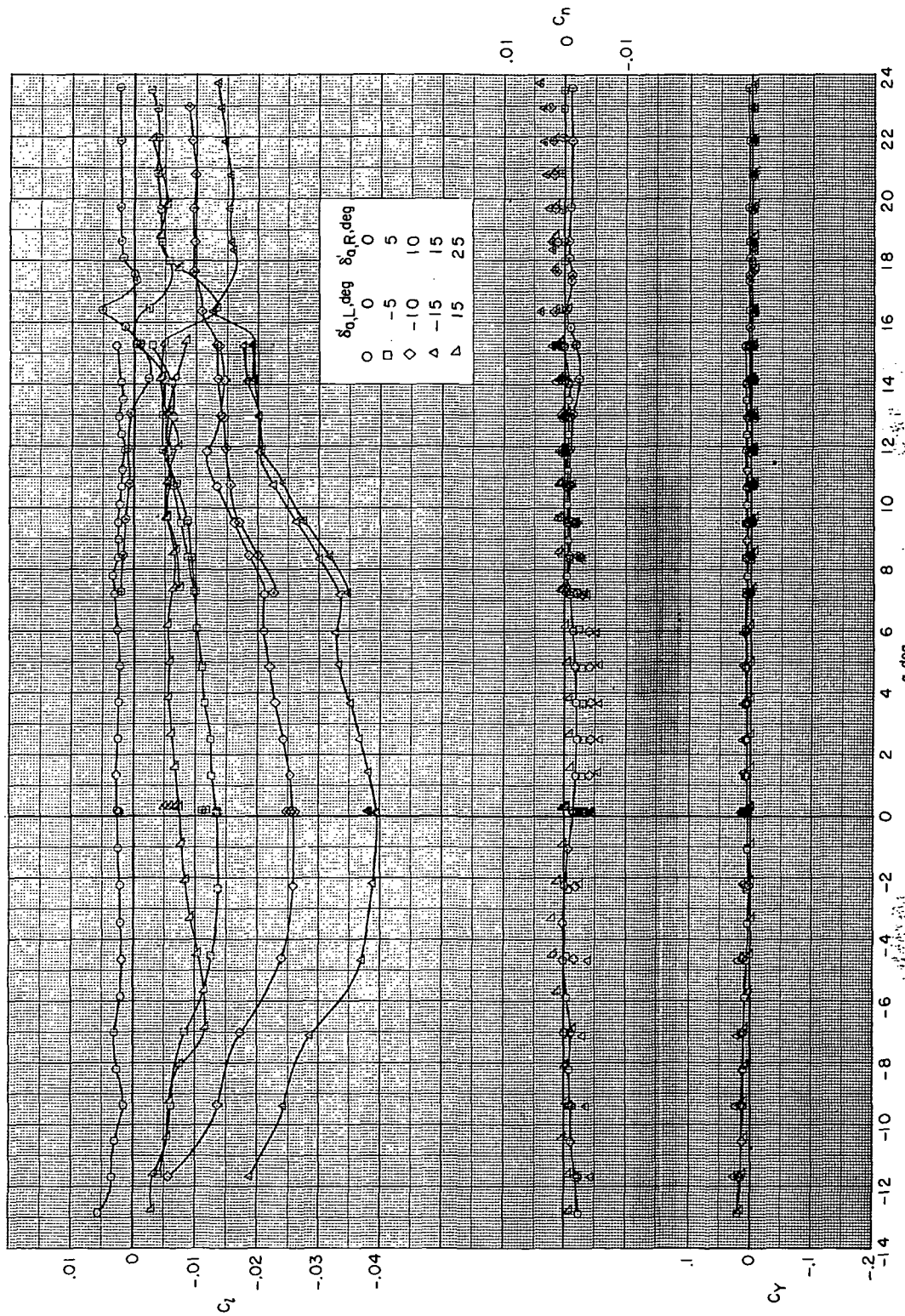

(b) M = 0.50.

Figure 5.- Continued.

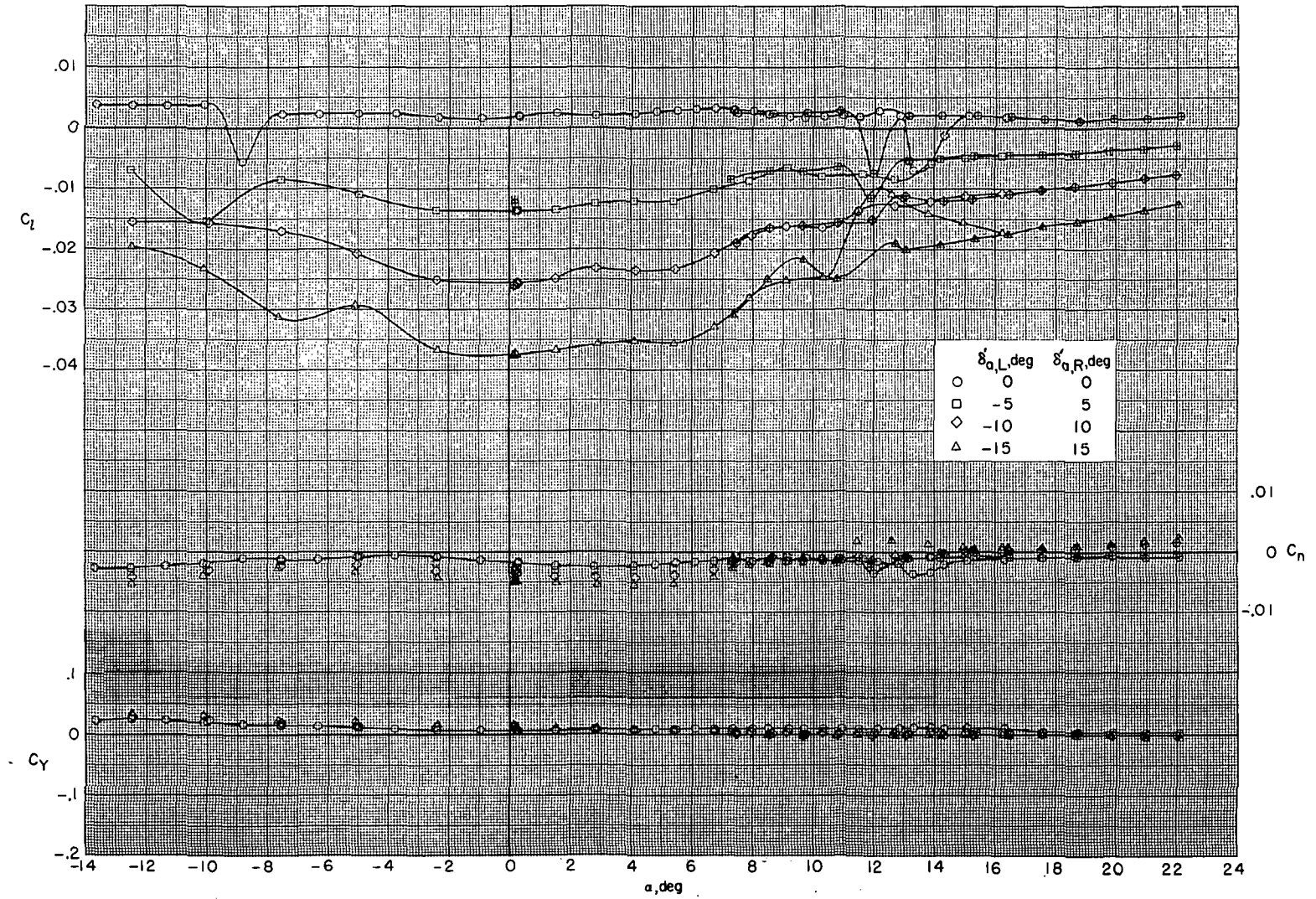

(c) M = 0.80.

Figure 5.- Continued.

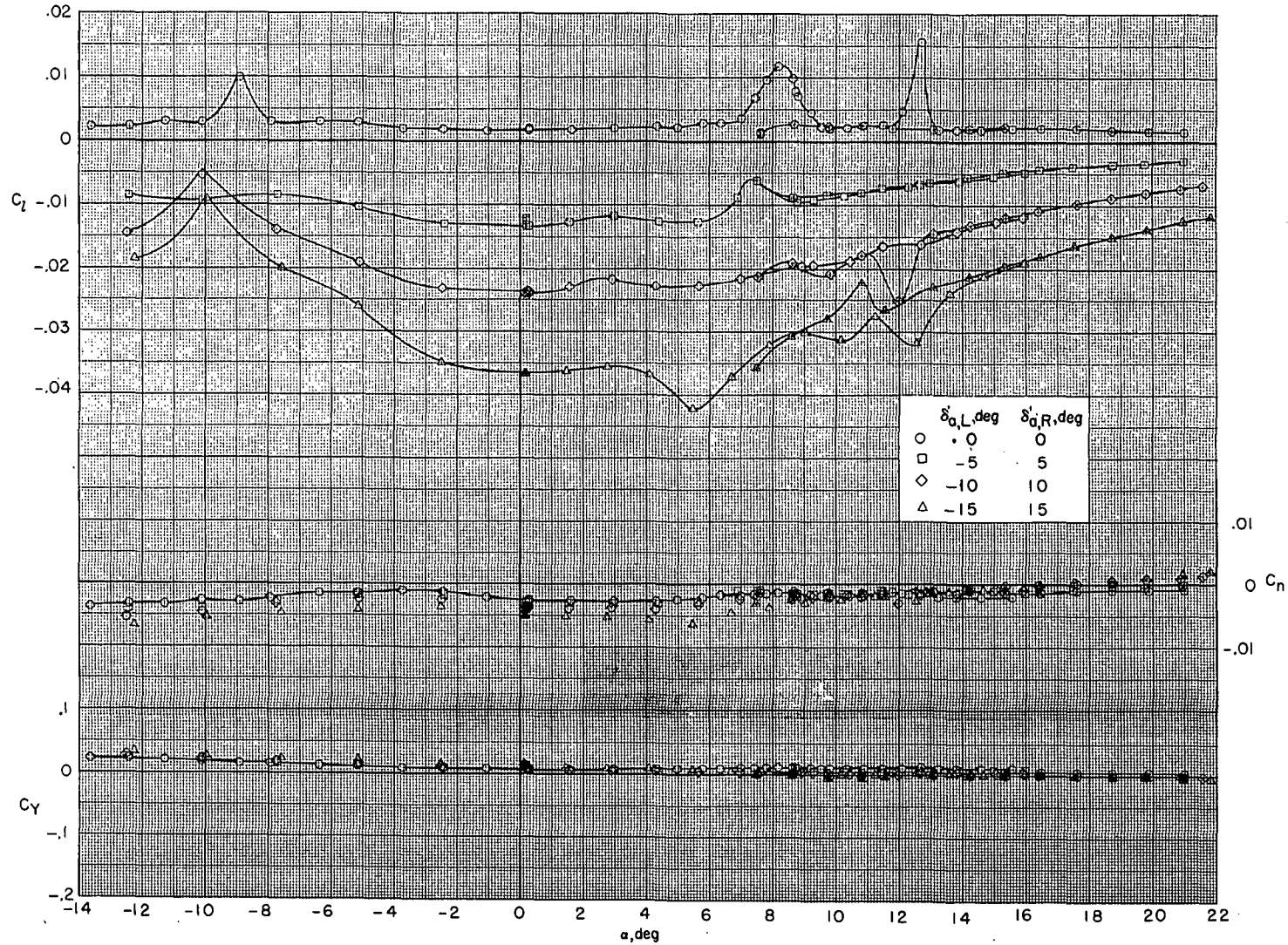

(d) M = 0.90.

Figure 5.- Continued.

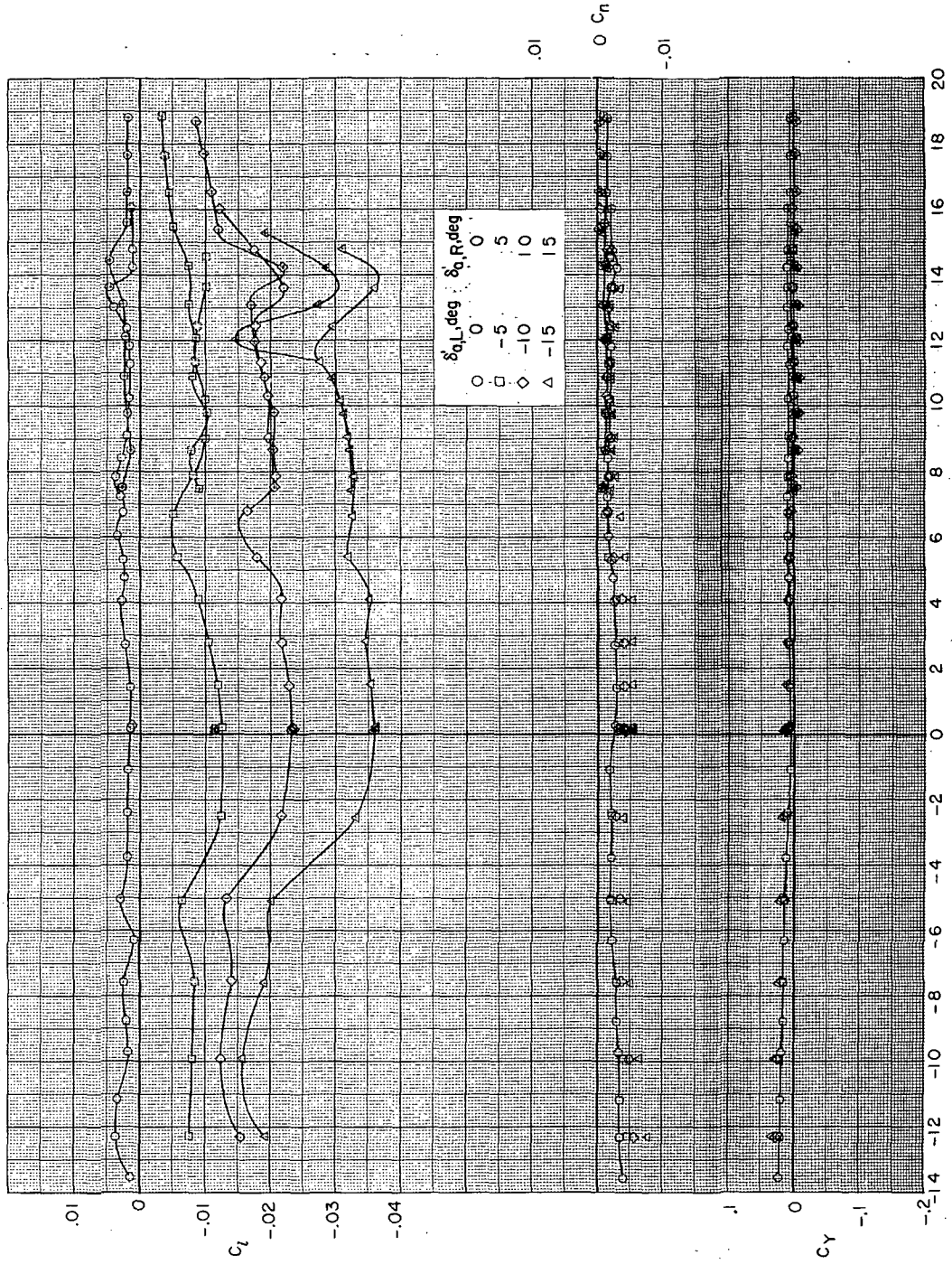

(e) M = 0.95.

Figure 5.- Continued.

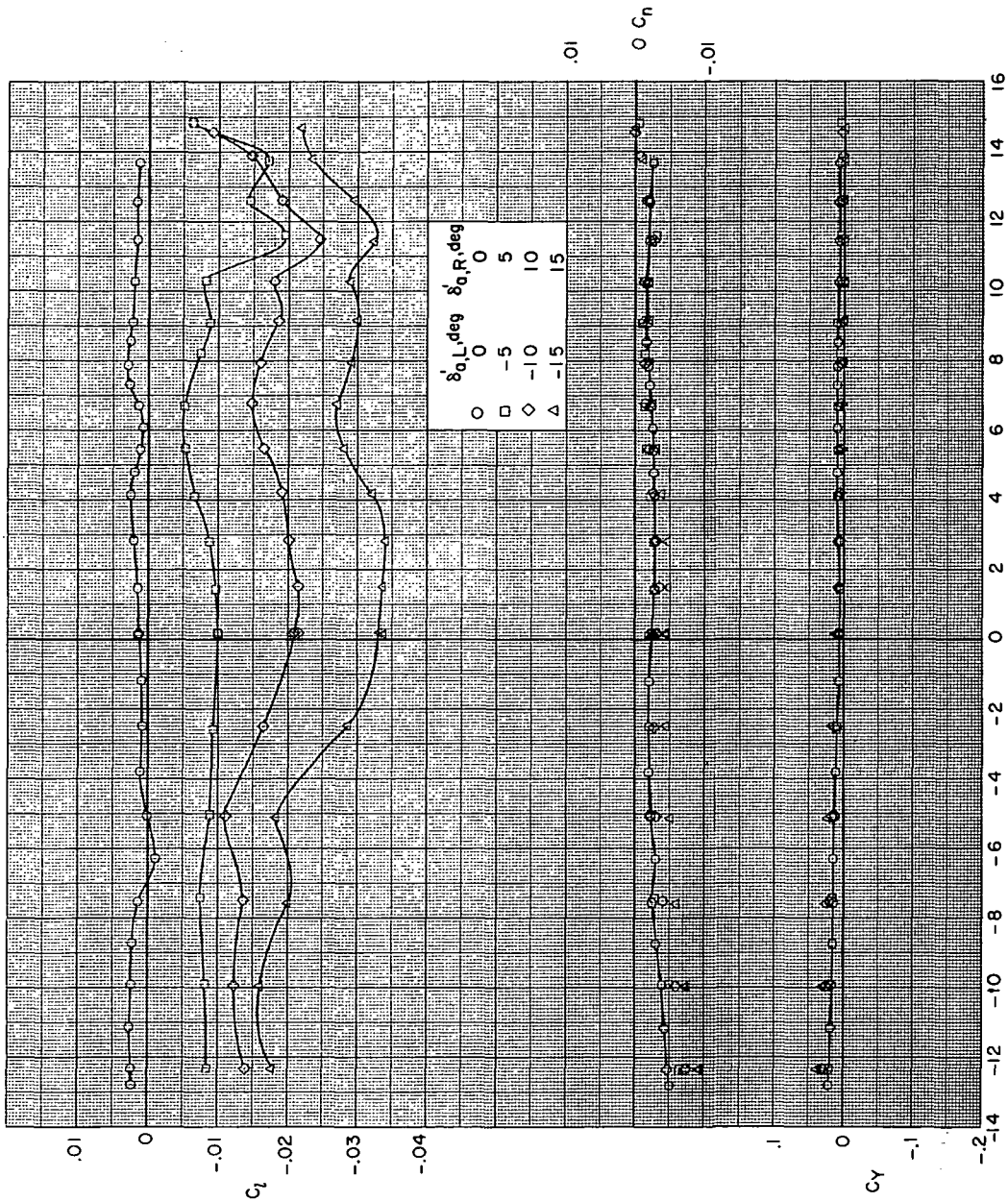

(f) M = 0.99.

Figure 5.- Concluded.

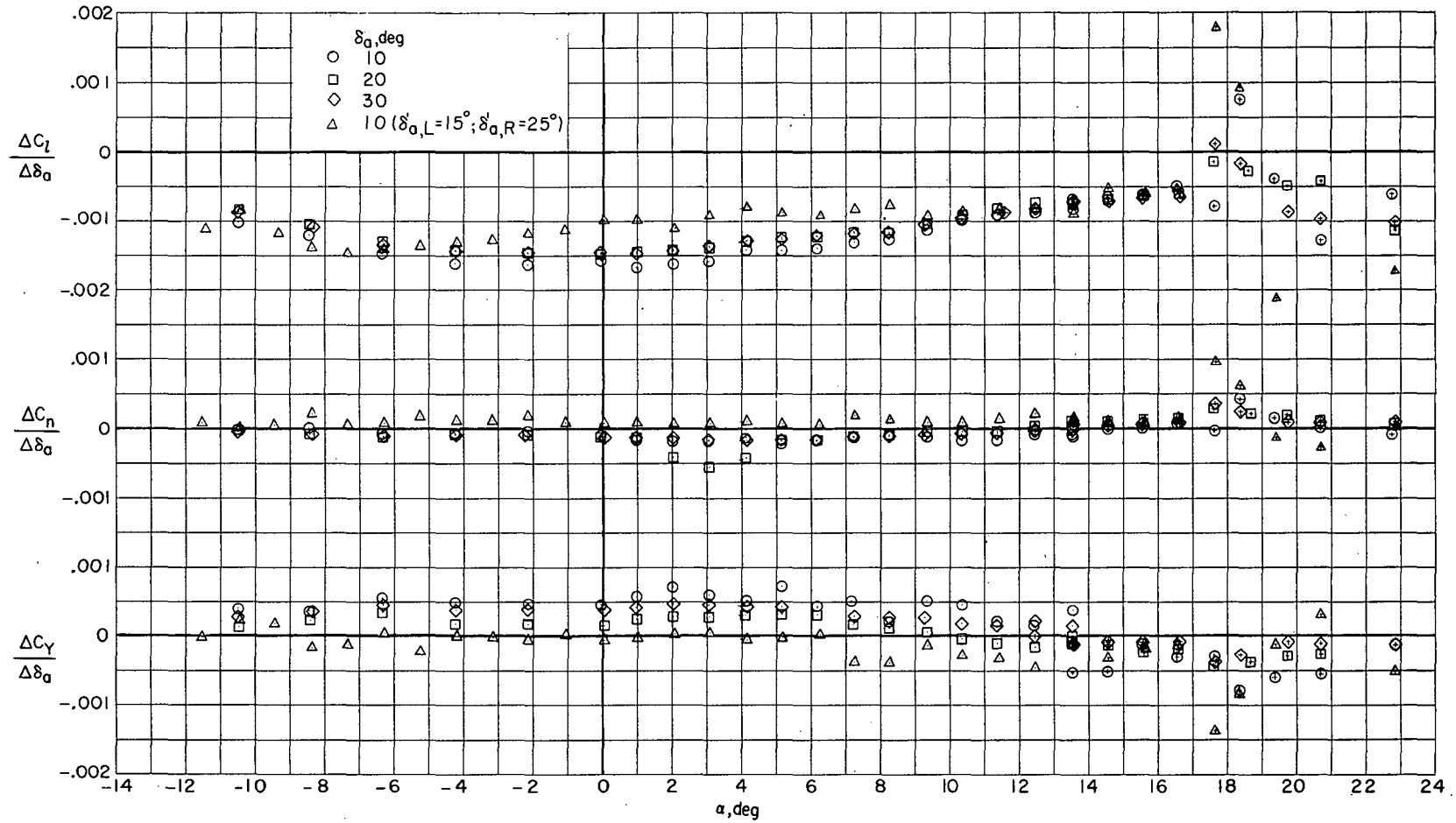

(a) M = 0.25.

Figure 6.- Variation with angle of attack of the lateral-directional aileron-control parameters: $\frac{\Delta C_l}{\Delta \delta a}$, $\frac{\Delta C_n}{\Delta \delta a}$, and $\frac{\Delta C_Y}{\Delta \delta a}$. $\delta_h = -2.5^o$.

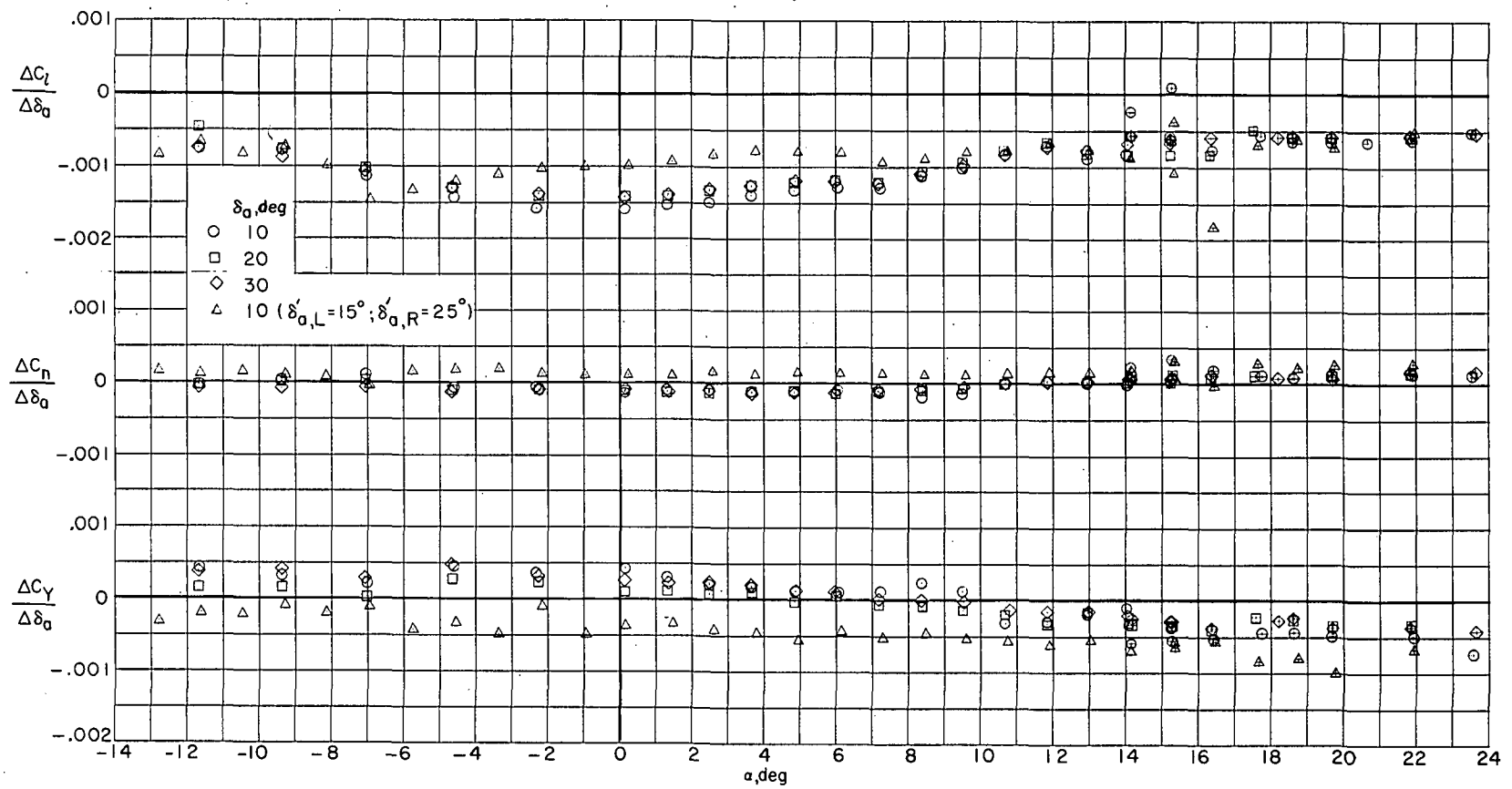

(b) M = 0.50.

Figure 6.- Continued.

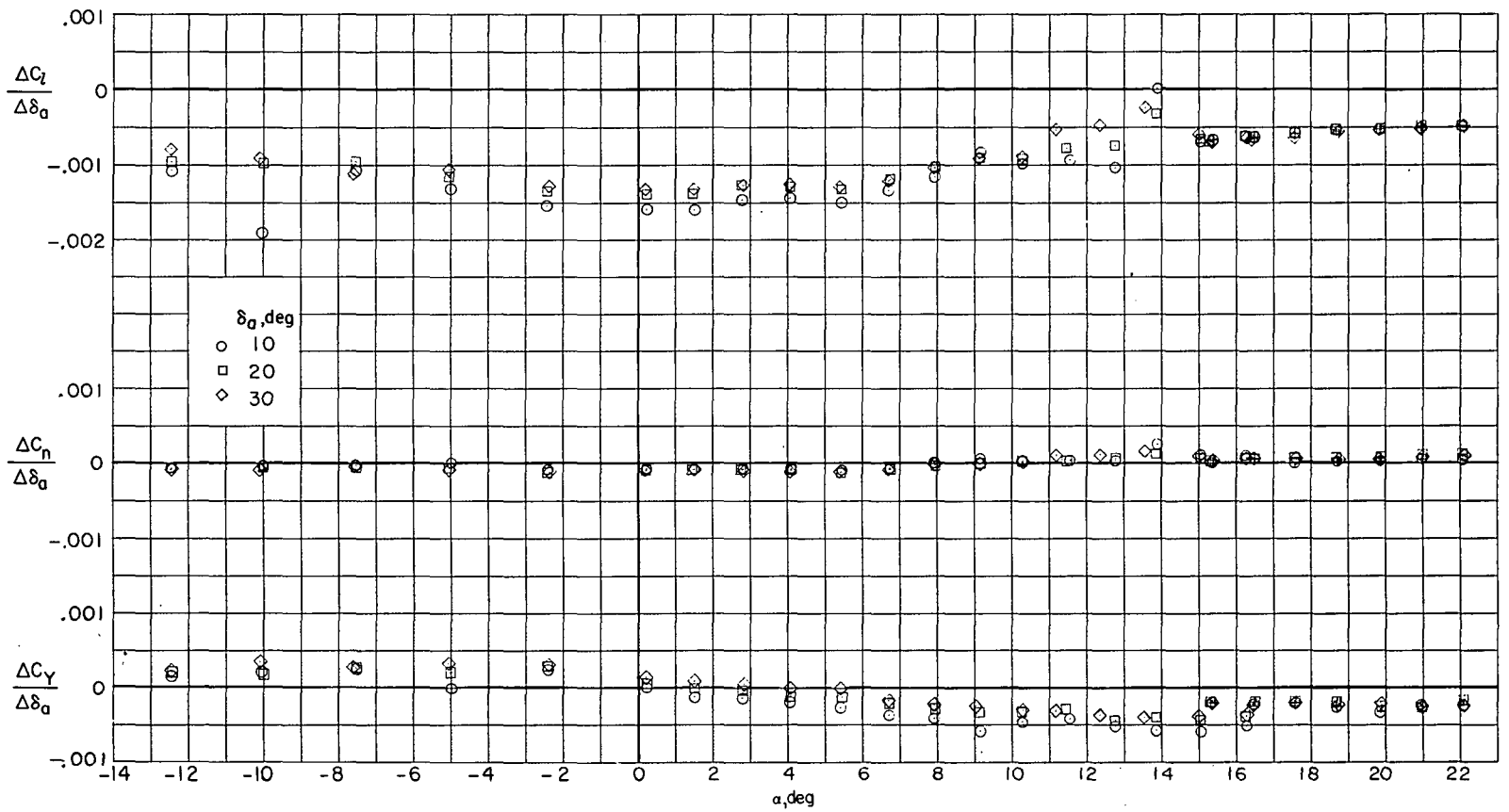

(c) M = 0.80.

Figure 6.- Continued.

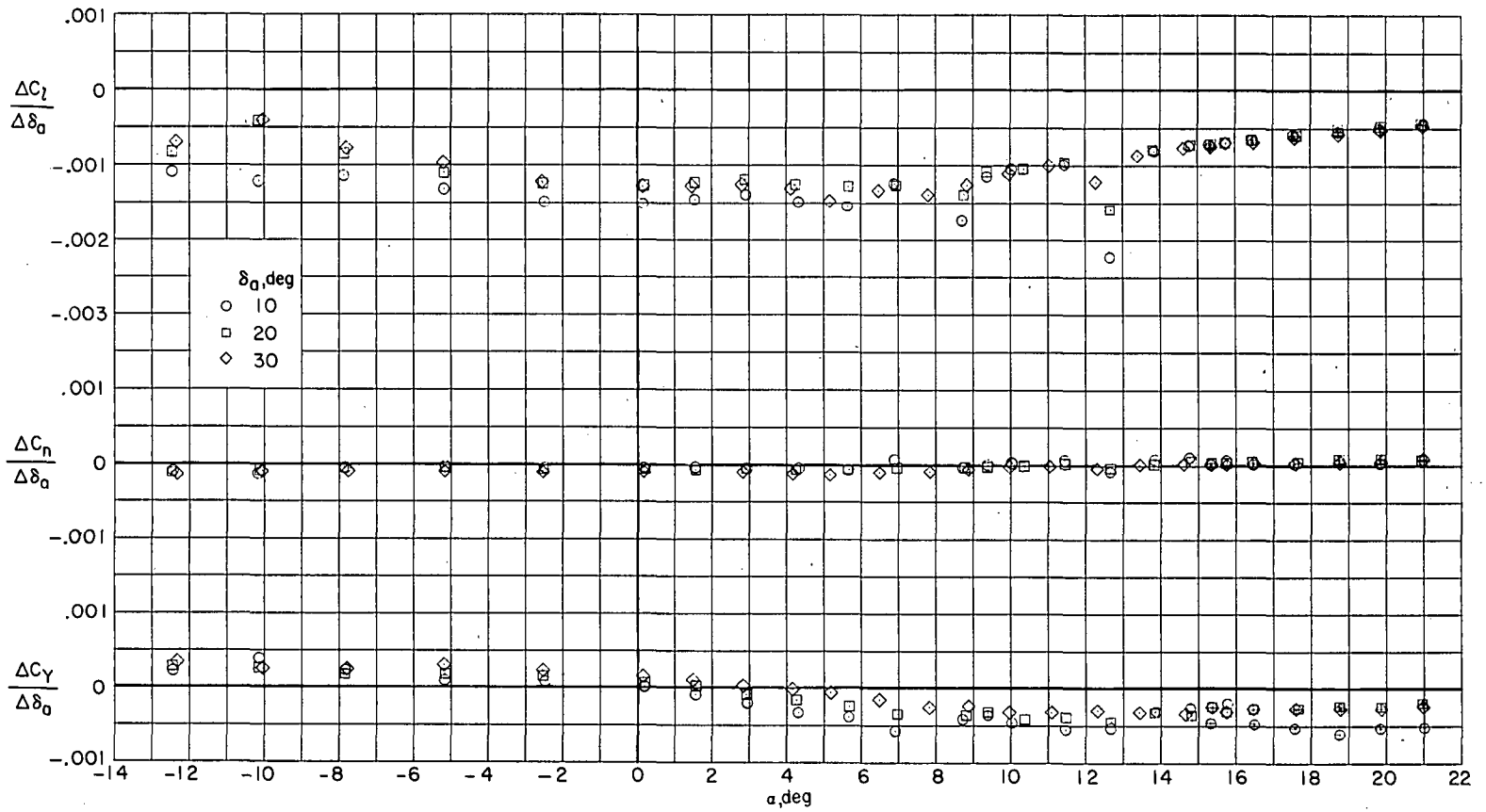

(d) M = 0.90.

Figure 6.- Continued.

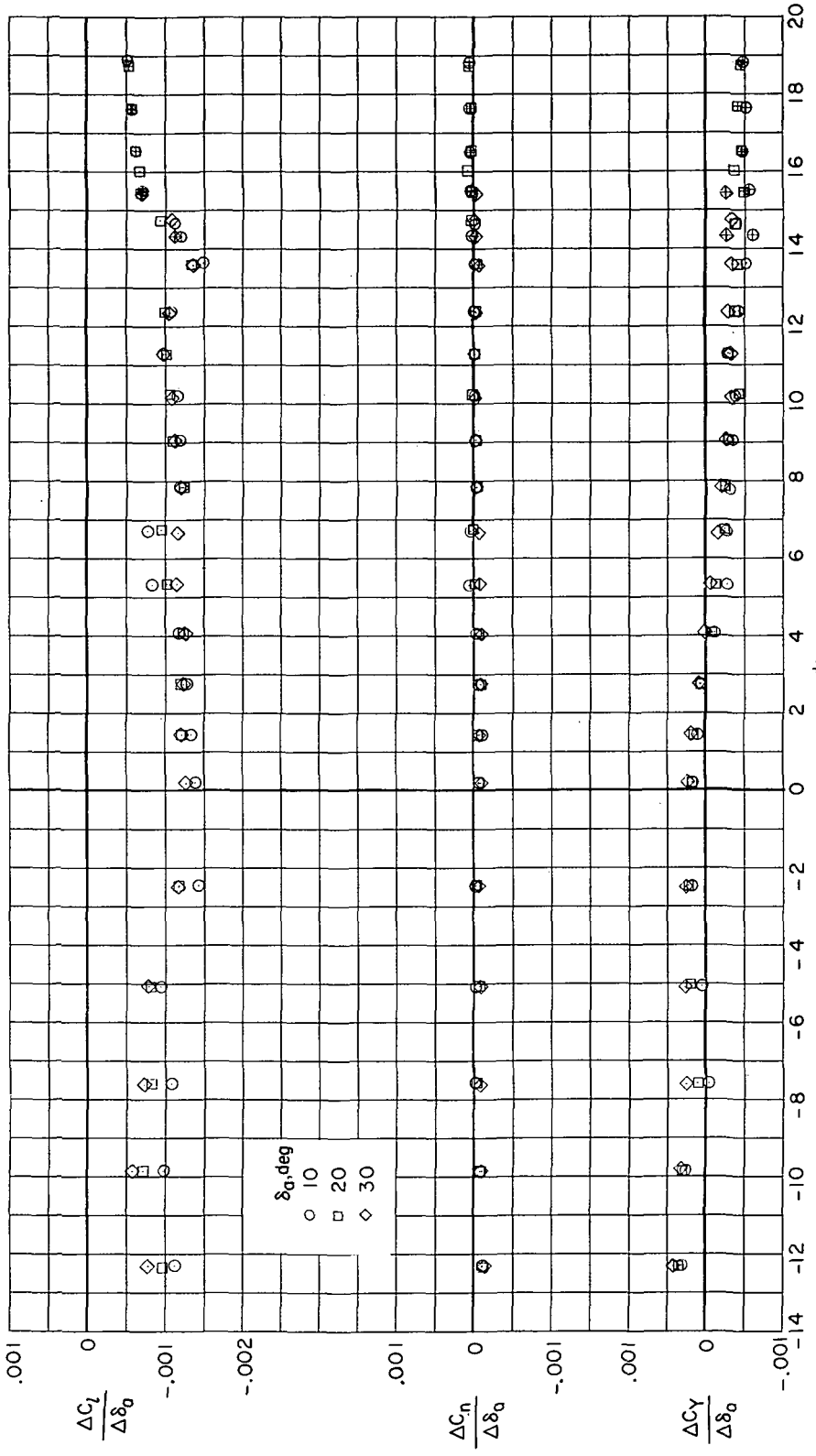

(e) M = 0.95.

Figure 6.- Continued.

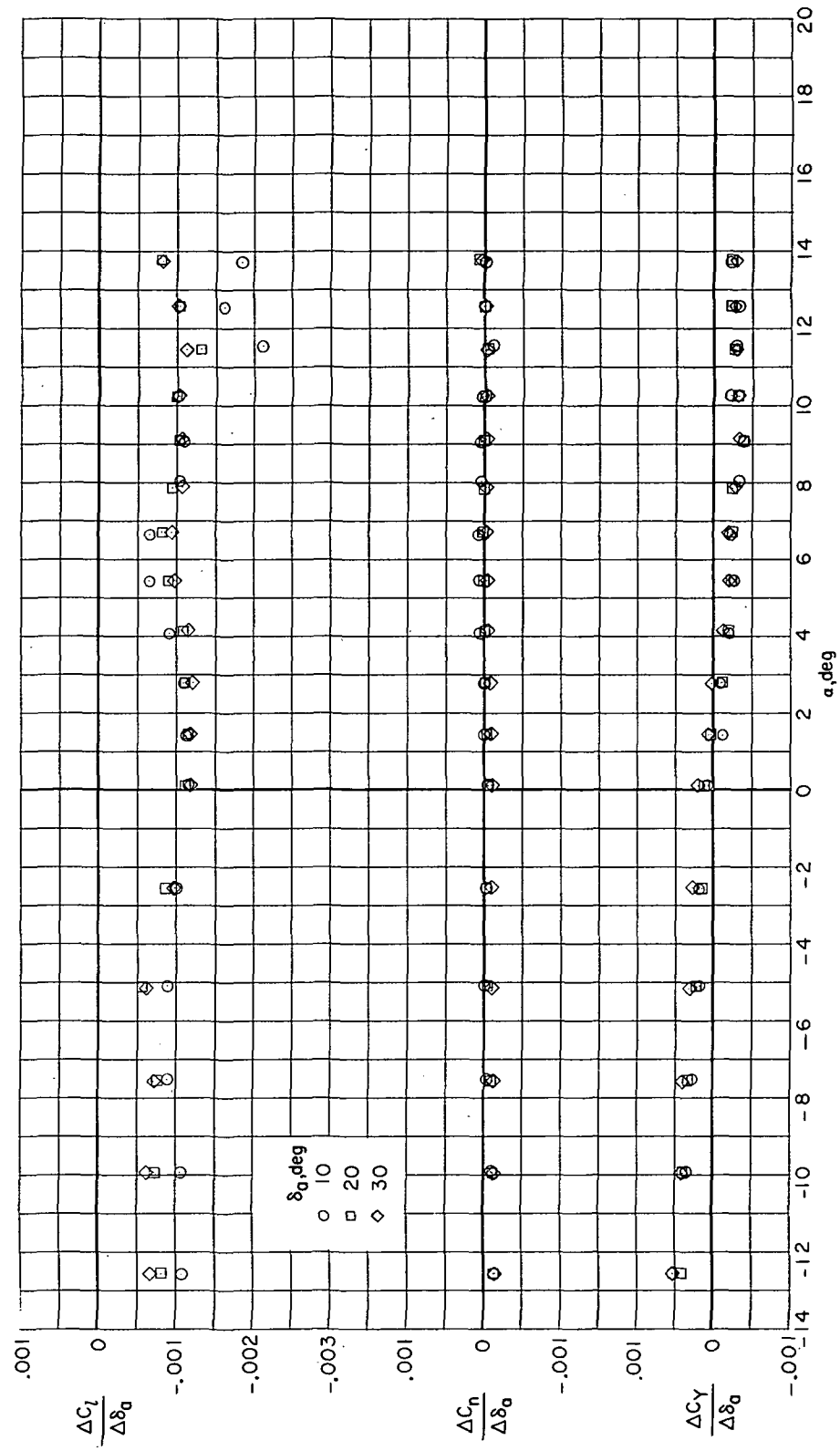

(f) M = 0.99.

Figure 6.- Concluded.

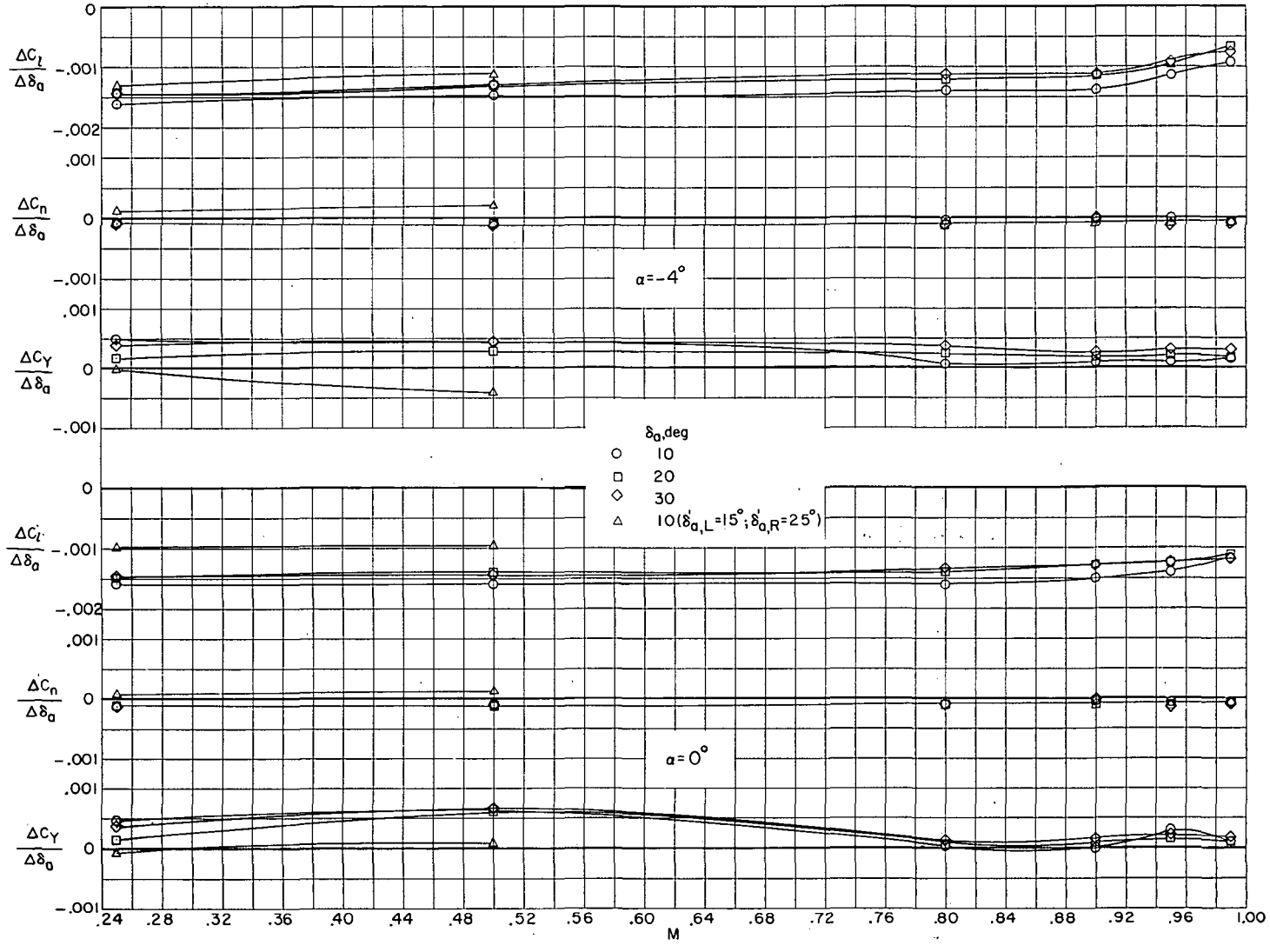

Figure 7.- Variation with Mach number of the lateral-directional aileron-control parameters: $\frac{\Delta C_l}{\Delta \delta_a}$, $\frac{\Delta C_n}{\Delta \delta_a}$, and $\frac{\Delta C_Y}{\Delta \delta_a}$. $\delta_h = -2.5^o$.

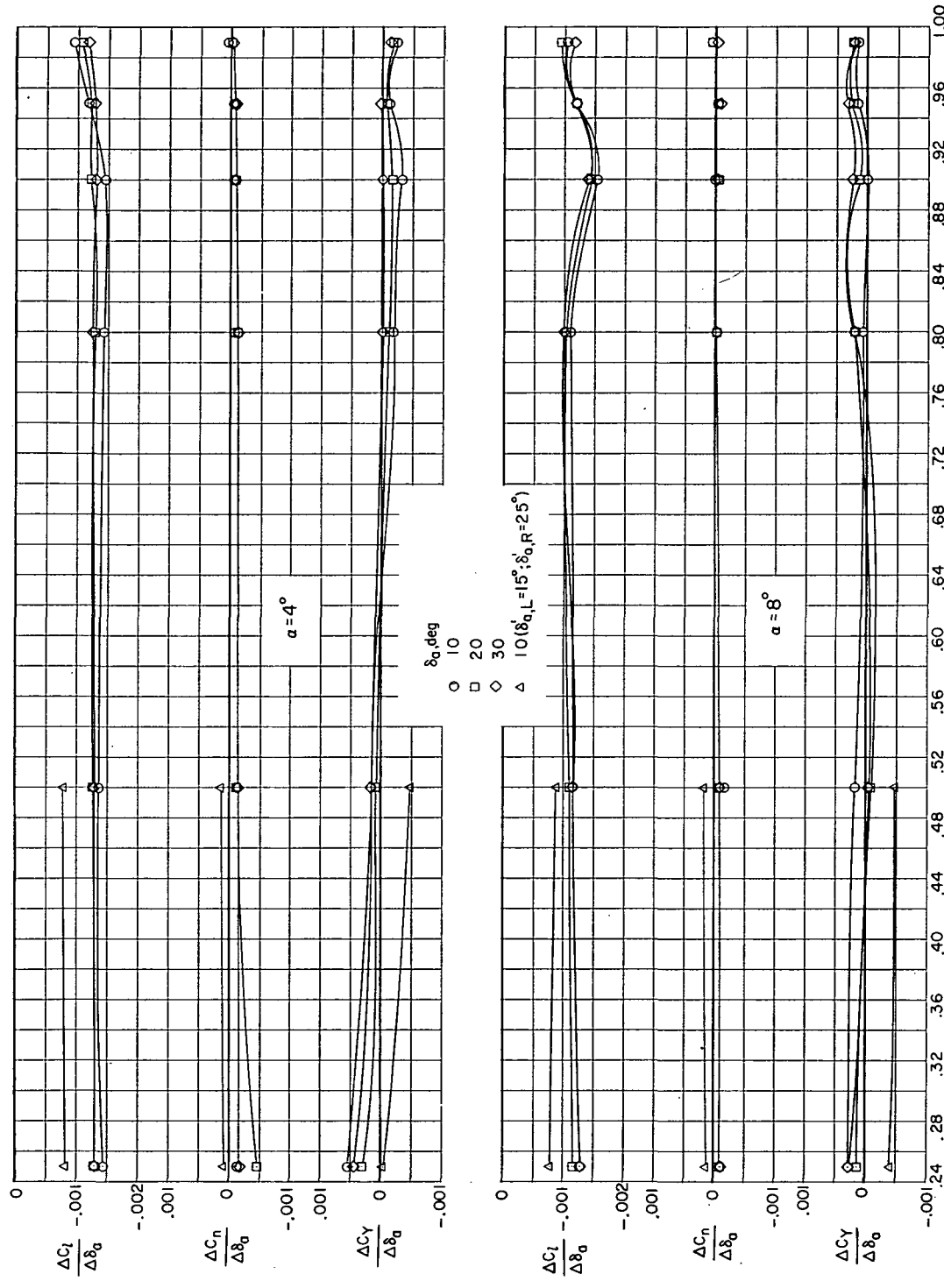

Figure 7.- Continued.

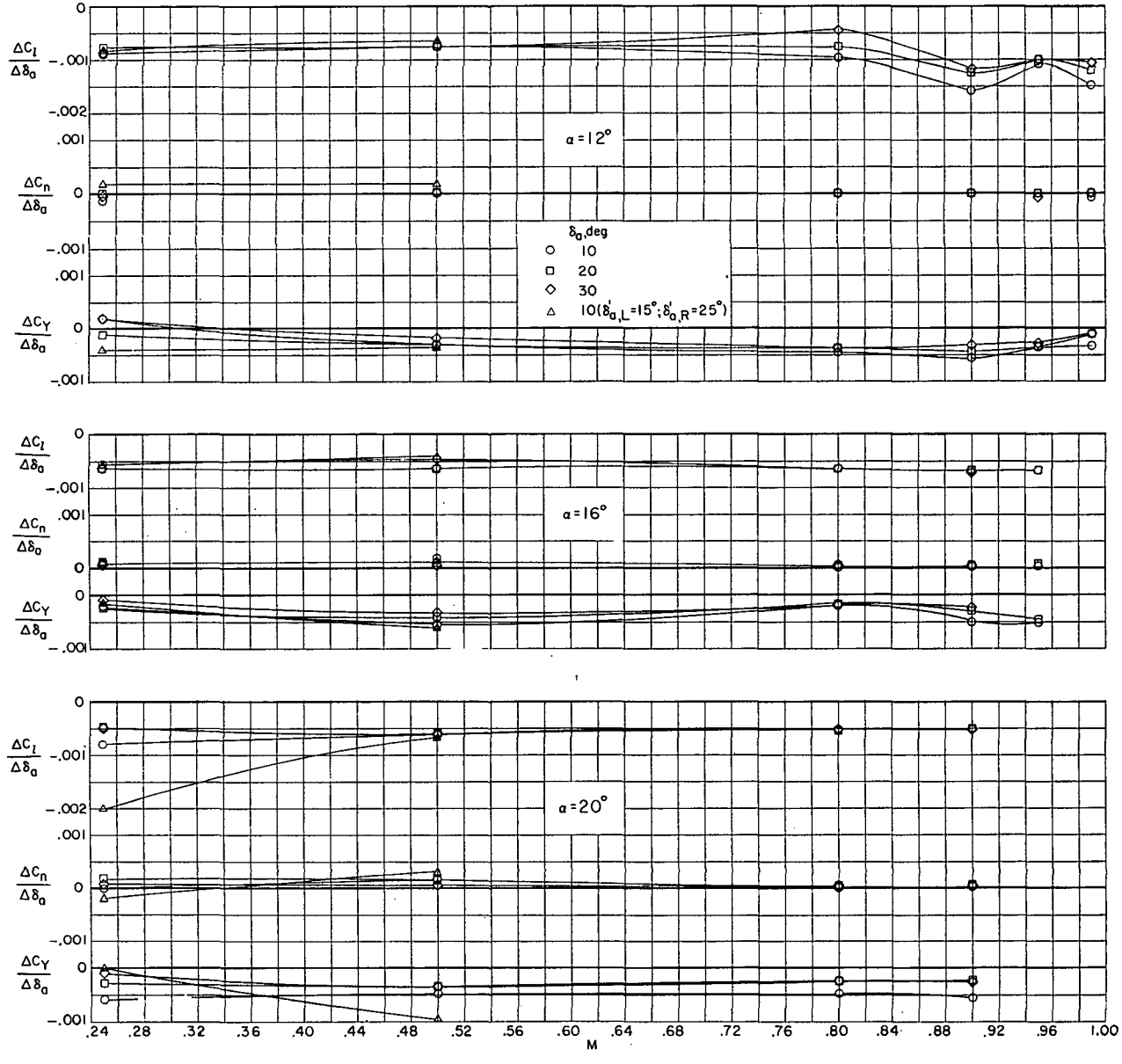

Figure 7.- Concluded.

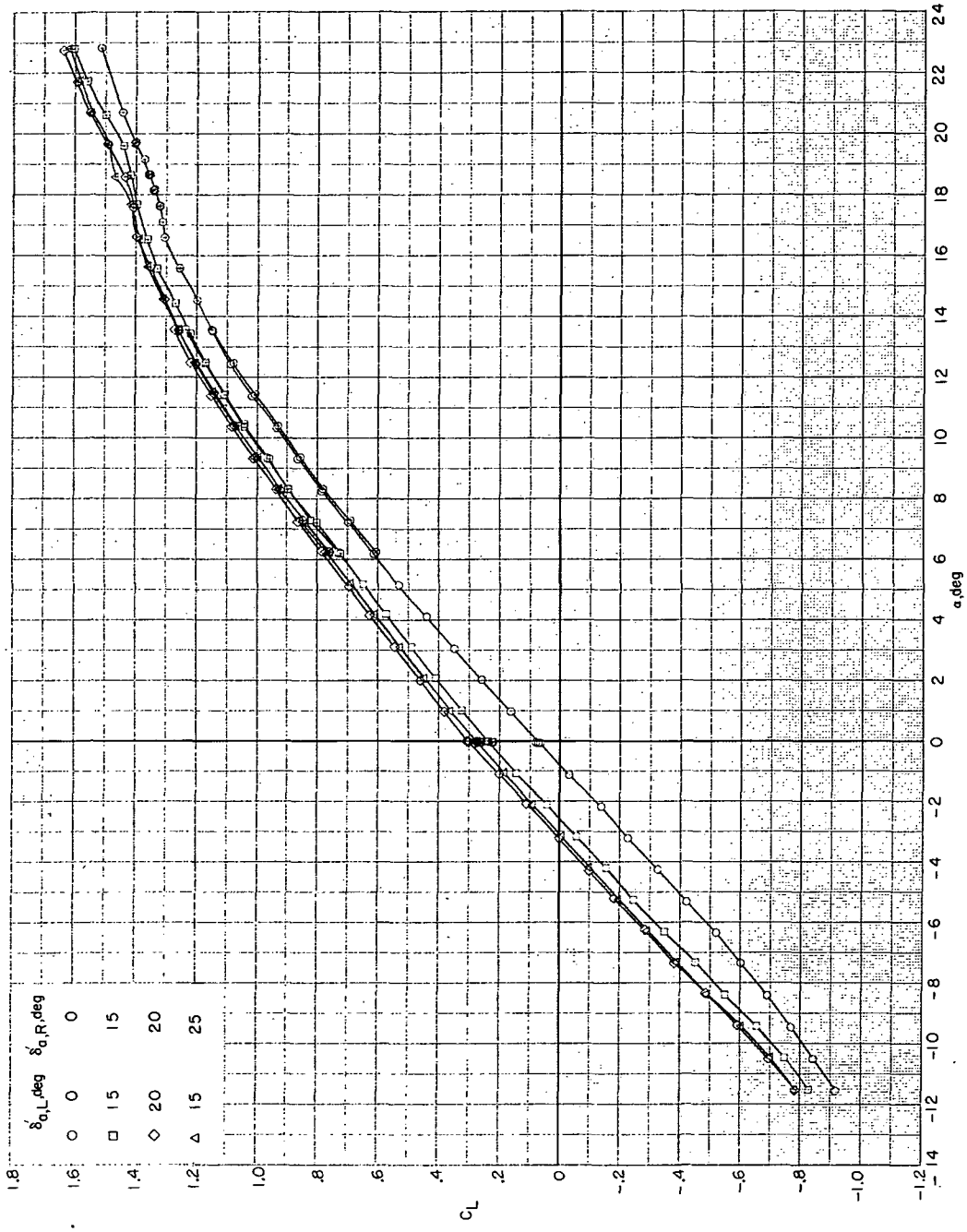

(a) M = 0.25.

Figure 8.- Effect of symmetrical aileron (flap) deflection on the longitudinal aerodynamic coefficients. $\delta_h = -2.5°$.

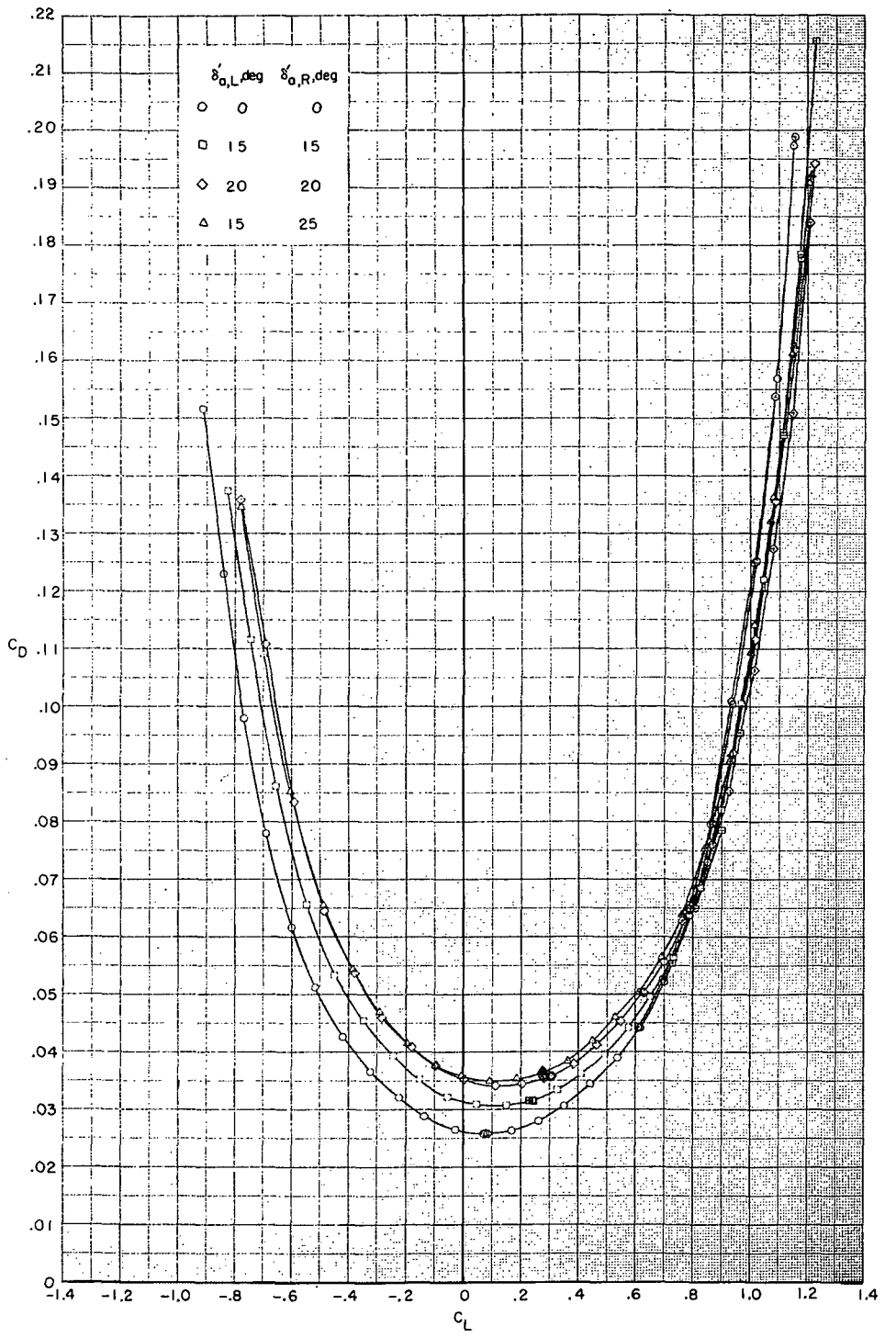

(a) M = 0.25. Continued.

Figure 8.- Continued.

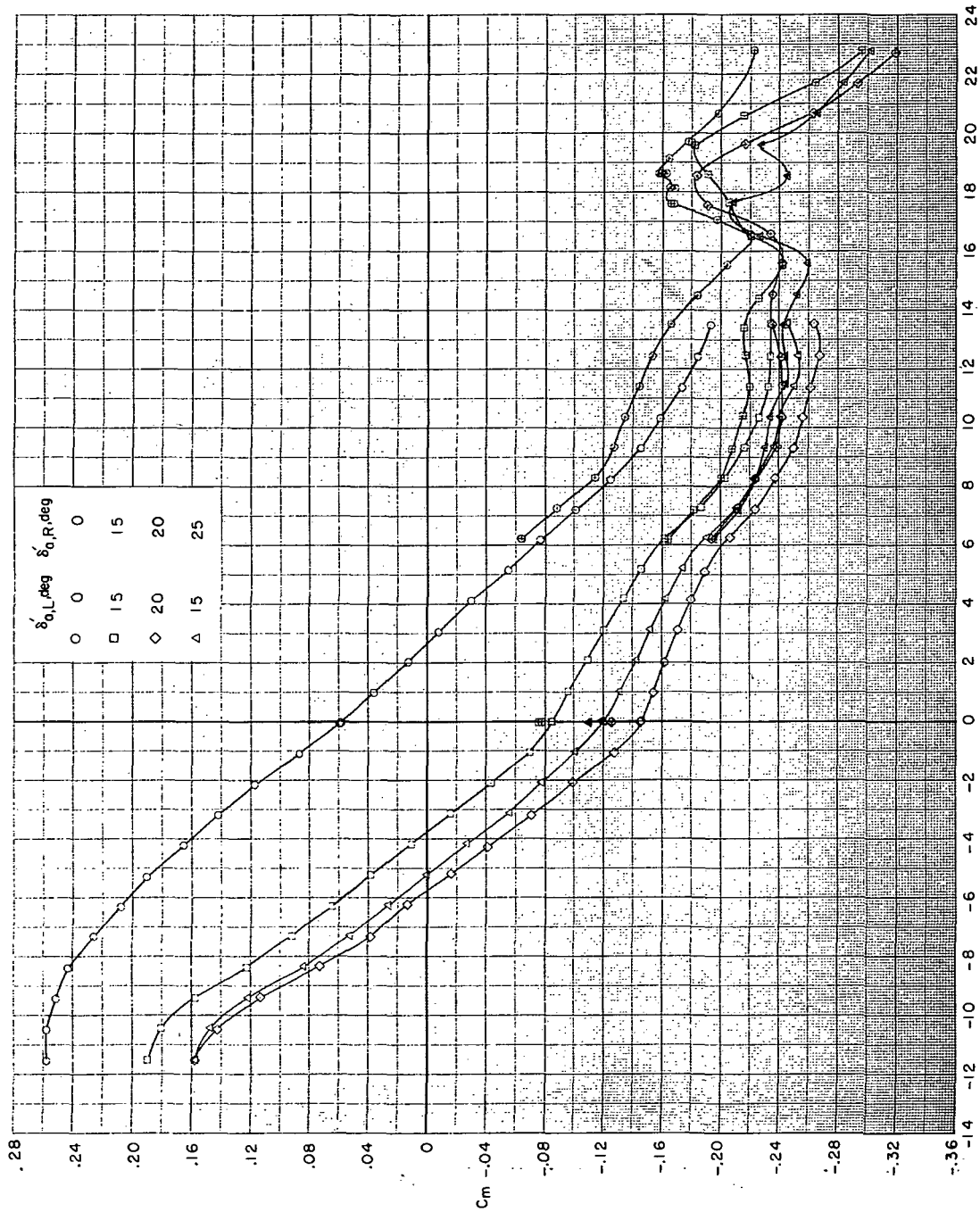

(a) M = 0.25. Continued.

Figure 8.- Continued.

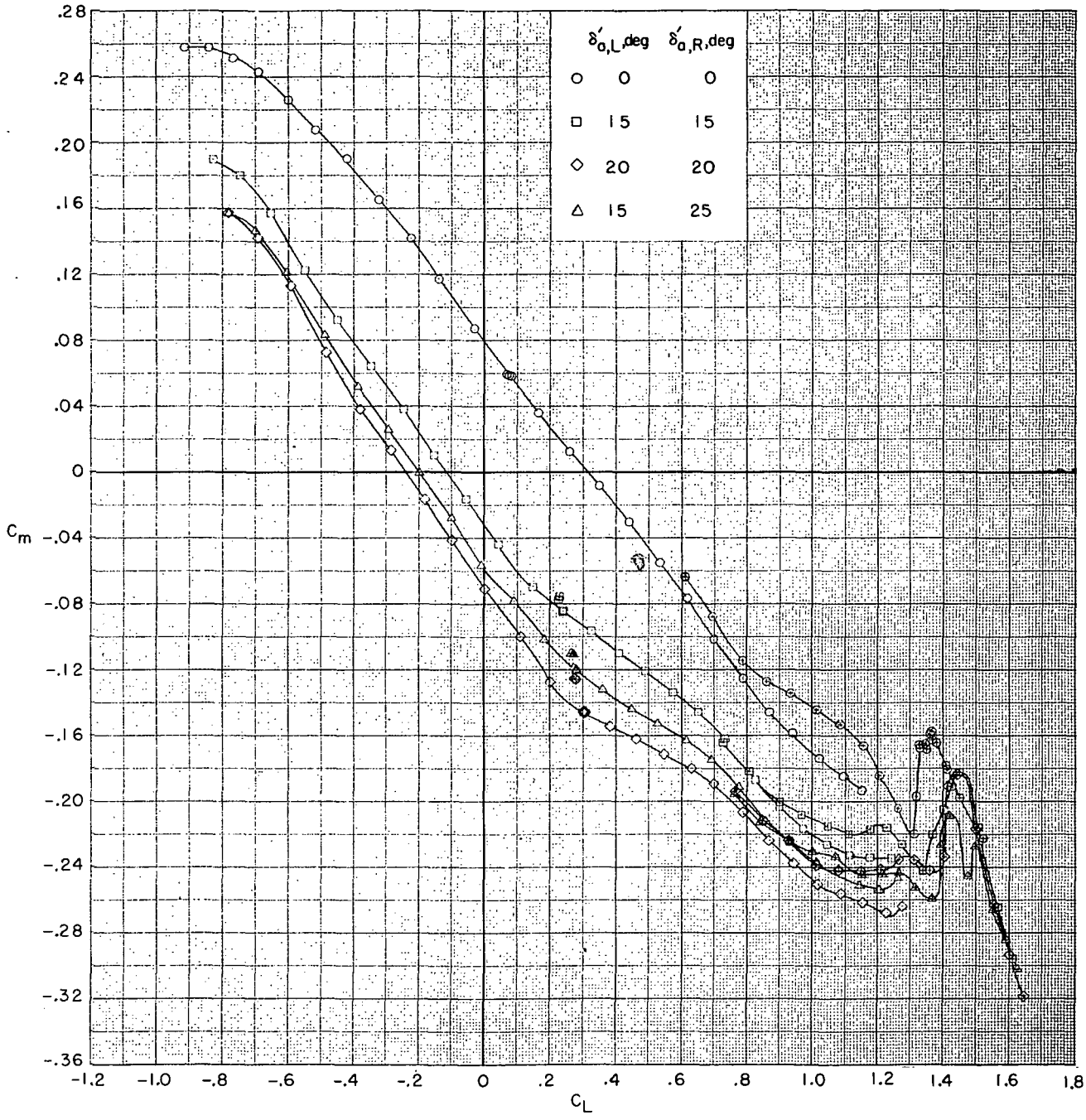

(a) M = 0.25. Concluded.

Figure 8.- Continued.

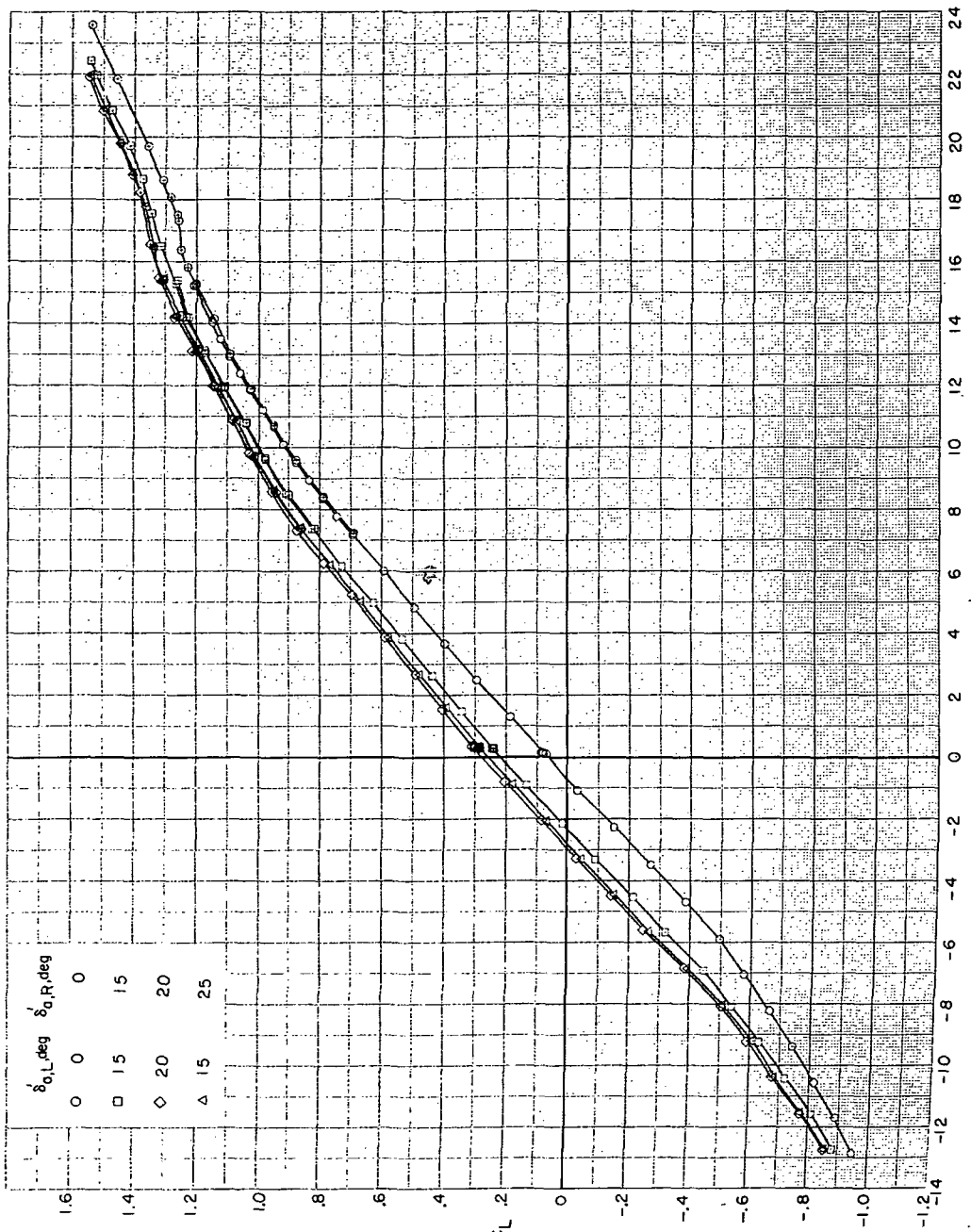

(b) M = 0.50.

Figure 8.- Continued.

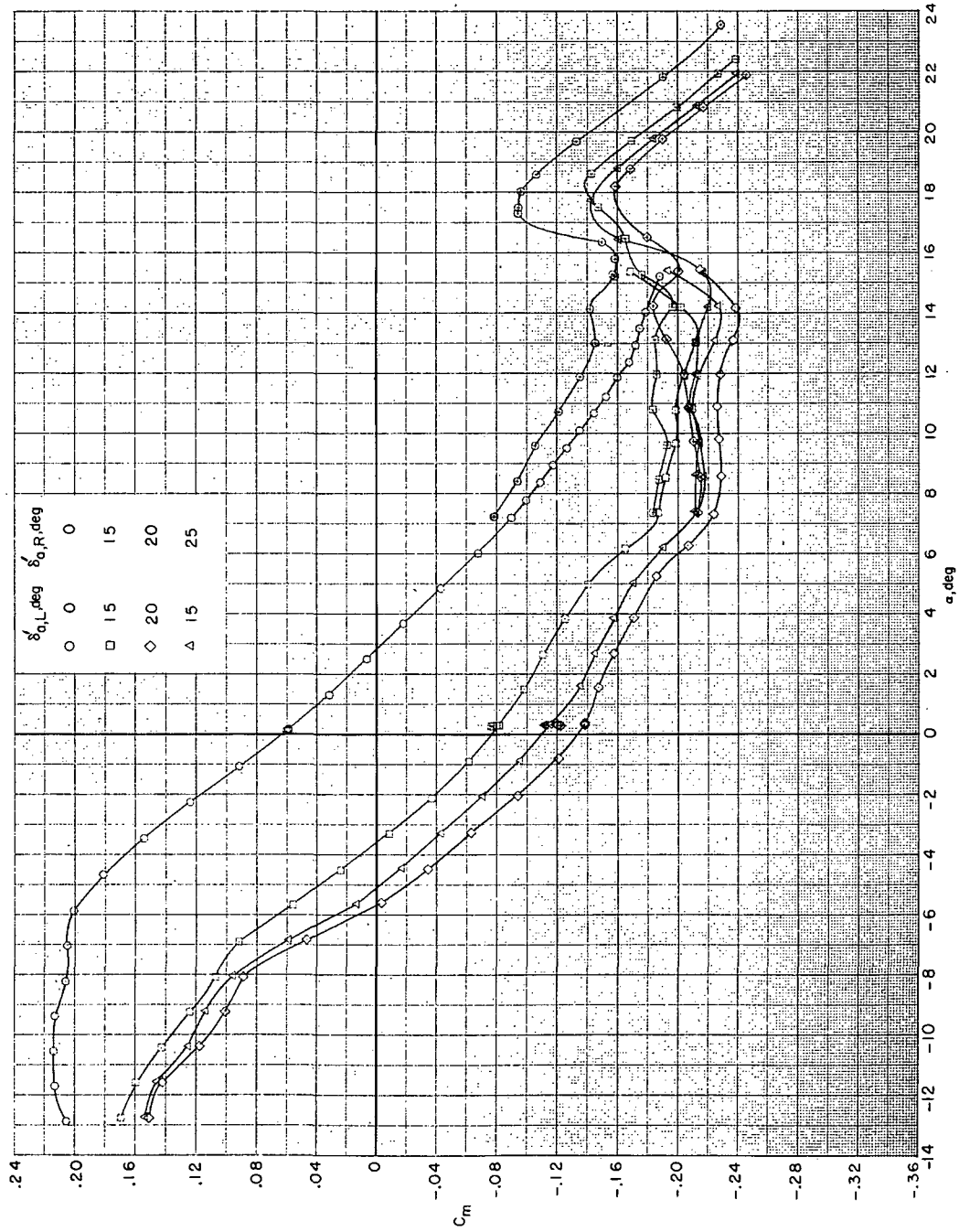

(b) M = 0.50. Continued.

Figure 8.- Continued.

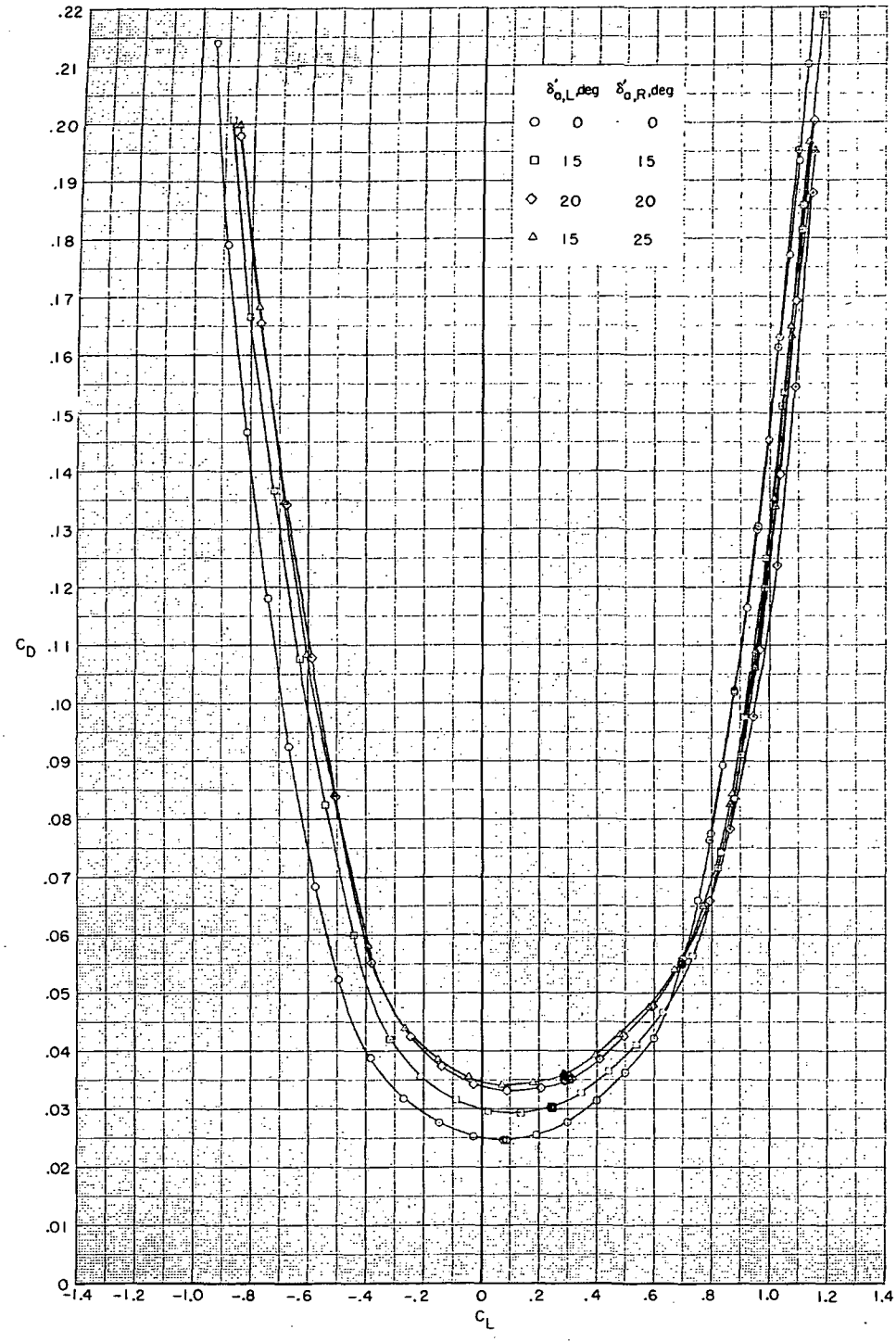

(b) M = 0.50. Continued.

Figure 8.- Continued.

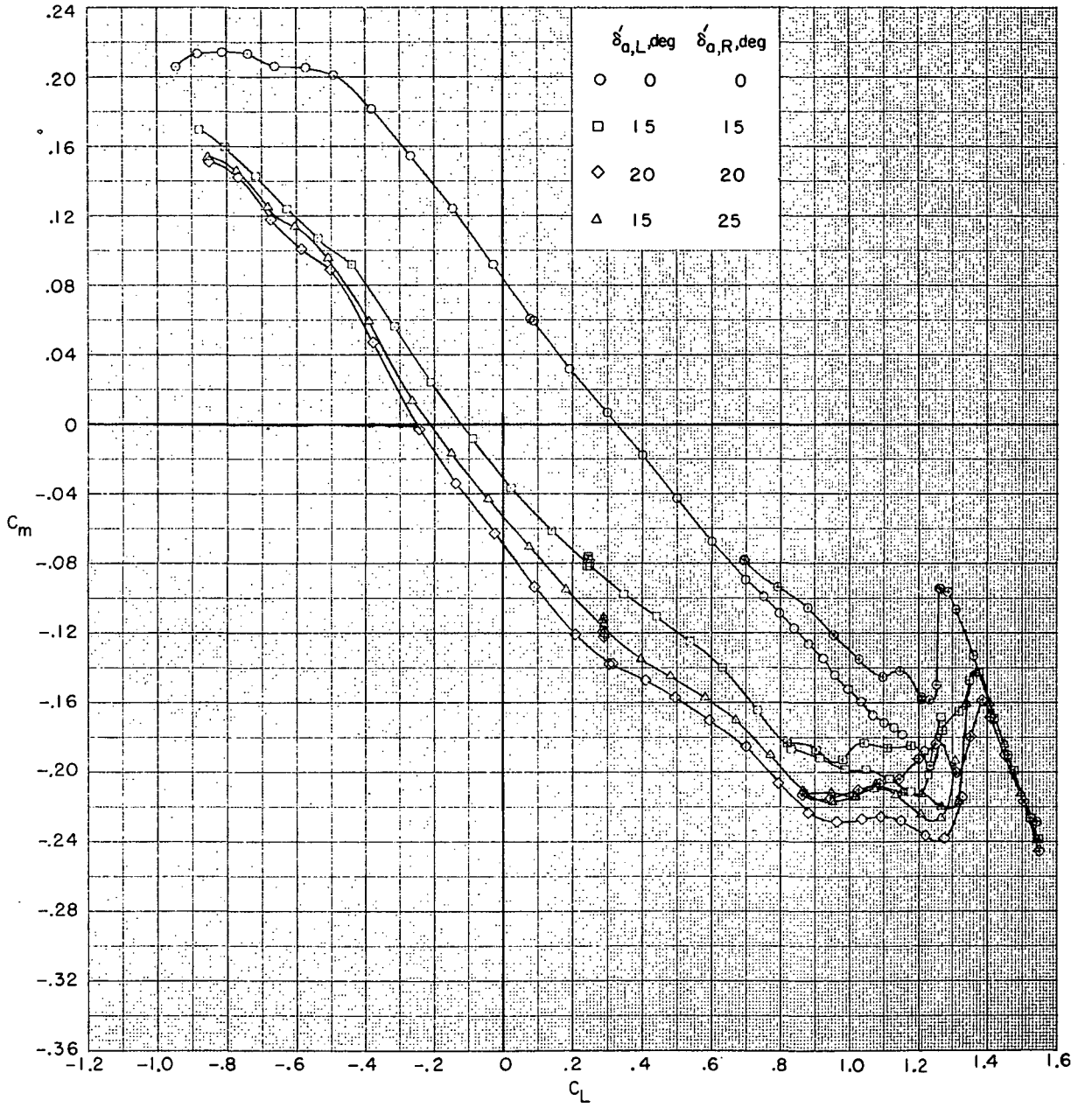

(b) M = 0.50. Concluded.

Figure 8.- Concluded.

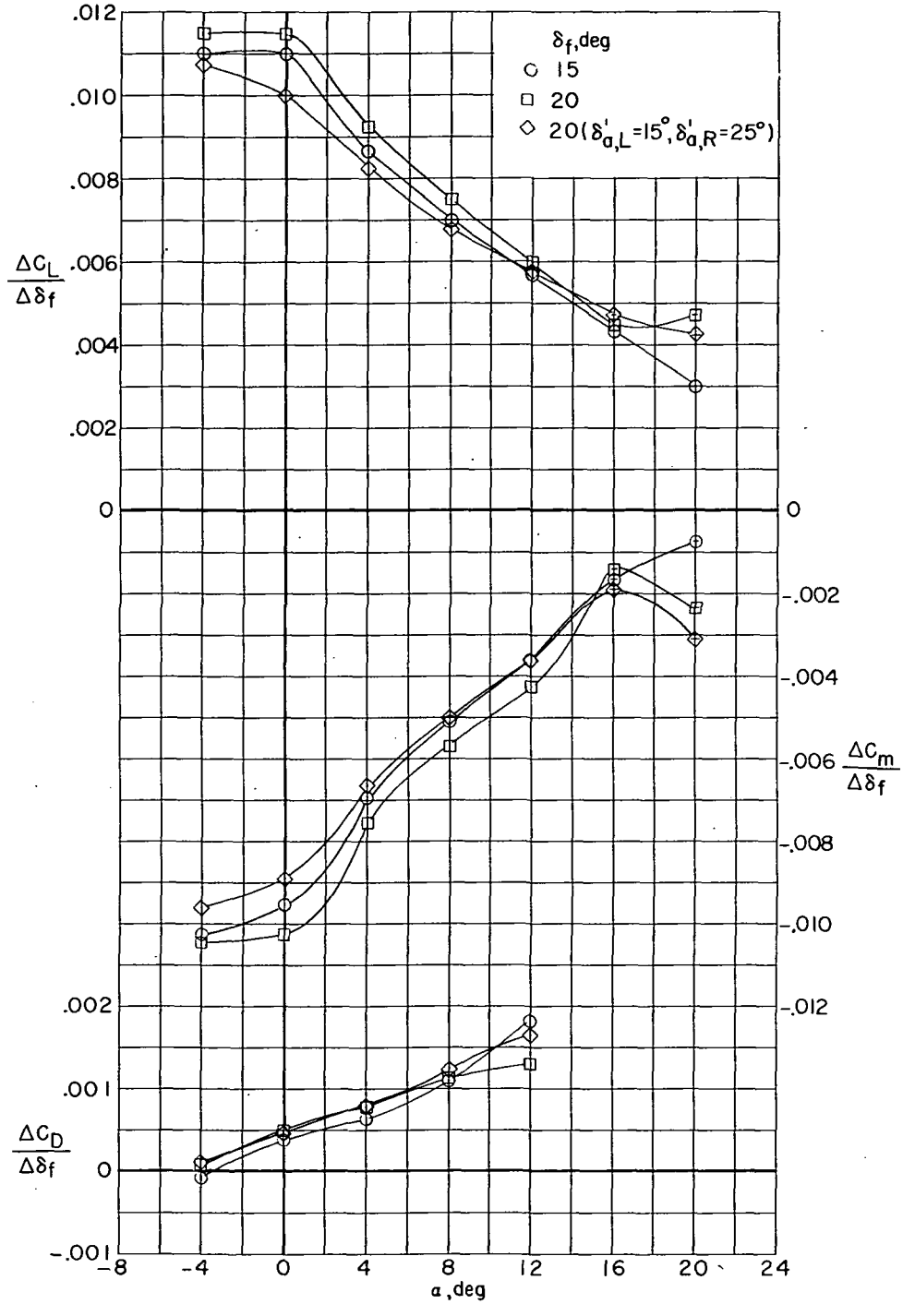

(a) M = 0.25.

Figure 9.- Variation with angle of attack of the longitudinal flap-control (symmetrical aileron deflection) parameters: $\frac{\Delta C_L}{\Delta \delta_f}$, $\frac{\Delta C_m}{\Delta \delta_f}$, and $\frac{\Delta C_D}{\Delta \delta_f}$. $\delta_h = -2.5^o$.

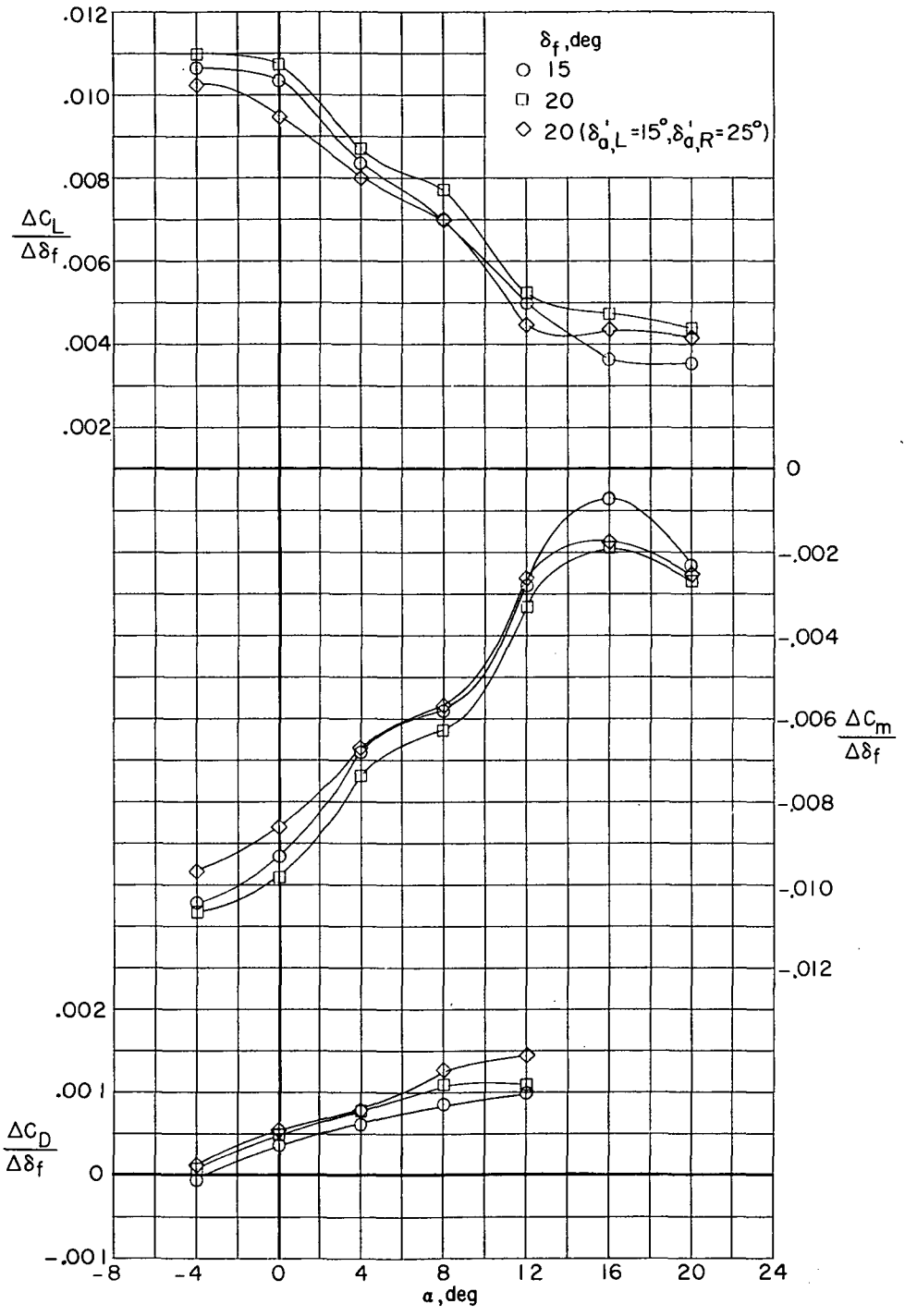

(b) M = 0.50.

Figure 9.- Concluded.

"The aeronautical and space activities of the United States shall be conducted so as to contribute . . . to the expansion of human knowledge of phenomena in the atmosphere and space. The Administration shall provide for the widest practicable and appropriate dissemination of information concerning its activities and the results thereof."

—NATIONAL AERONAUTICS AND SPACE ACT OF 1958

NASA SCIENTIFIC AND TECHNICAL PUBLICATIONS

TECHNICAL REPORTS: Scientific and technical information considered important, complete, and a lasting contribution to existing knowledge.

TECHNICAL NOTES: Information less broad in scope but nevertheless of importance as a contribution to existing knowledge.

TECHNICAL MEMORANDUMS: Information receiving limited distribution because of preliminary data, security classification, or other reasons.

CONTRACTOR REPORTS: Scientific and technical information generated under a NASA contract or grant and considered an important contribution to existing knowledge.

TECHNICAL TRANSLATIONS: Information published in a foreign language considered to merit NASA distribution in English.

SPECIAL PUBLICATIONS: Information derived from or of value to NASA activities. Publications include conference proceedings, monographs, data compilations, handbooks, sourcebooks, and special bibliographies.

TECHNOLOGY UTILIZATION PUBLICATIONS: Information on technology used by NASA that may be of particular interest in commercial and other non-aerospace applications. Publications include Tech Briefs, Technology Utilization Reports and Notes, and Technology Surveys.

Details on the availability of these publications may be obtained from:

SCIENTIFIC AND TECHNICAL INFORMATION OFFICE

NATIONAL AERONAUTICS AND SPACE ADMINISTRATION

Washington, D.C. 20546